

Spin Pumping and Spin Transfer

Arne Brataas¹, Yaroslav Tserkovnyak², Gerrit E. W. Bauer^{3,4}, and Paul J. Kelly⁵

¹*Department of Physics, Norwegian University of Science and Technology, N-7491 Trondheim, Norway*

²*Department of Physics and Astronomy, University of California, Los Angeles, California, 900095, USA*

³*Delft University of Technology, Kavli Institute of NanoScience, 2628 CJ Delft, The Netherlands*

⁴*Institute for Materials Research, Tohoku University, Sendai 980-8577, Japan and*

⁵*Department of Applied Physics, Twente University, Enschede, The Netherlands*

Spin pumping is the emission of a spin current by a magnetization dynamics while spin transfer stands for the excitation of magnetization by spin currents. Using Onsager's reciprocity relations we prove that spin pumping and spin-transfer torques are two fundamentally equivalent dynamic processes in magnetic structures with itinerant electrons. We review the theory of the coupled motion of the magnetization order parameter and electron for textured bulk ferromagnets (*e.g.* containing domain walls) and heterostructures (such as spin valves). We present first-principles calculations for the material-dependent damping parameters of magnetic alloys. Theoretical and experimental results agree in general well.

Contents

I. Introduction	2
A. Technology Pull and Physics Push	2
B. Discrete versus Homogeneous	2
C. This Chapter	2
II. Phenomenology	3
A. Mechanics	3
B. Spin-transfer Torque and Spin-pumping	3
1. Discrete Systems	4
2. Continuous Systems	7
3. Self-consistency: Spin-battery and enhanced Gilbert Damping	8
C. Onsager Reciprocity Relations	9
1. Discrete Systems	9
2. Continuous Systems	11
III. Microscopic Derivations	12
A. Spin-transfer Torque	12
1. Discrete Systems - Magneto-electronic Circuit Theory	12
2. Continuous Systems	14
B. Spin Pumping	16
1. Discrete Systems	16
2. Continuous Systems	17
IV. First-principles Calculations	18
A. Alpha	19
1. NiFe alloys.	20
B. Beta	23
V. Theory versus Experiments	24
VI. Conclusions	25
Acknowledgments	25
References	26

I. INTRODUCTION

A. Technology Pull and Physics Push

The interaction between electric currents and the magnetic order parameter in conducting magnetic micro- and nanostructures has developed into a major subfield in magnetism¹. The main reason is the technological potential of magnetic devices based on transition metals and their alloys that operate at ambient temperatures. Examples are current-induced tunable microwave generators (spin-torque oscillators)^{2,3}, and non-volatile magnetic electronic architectures that can be randomly read, written or programmed by current pulses in a scalable manner⁴. The interaction between currents and magnetization can also cause undesirable effects such as enhanced magnetic noise in read heads made from magnetic multilayers⁵. While most research has been carried out on metallic structures, current-induced magnetization dynamics in semiconductors⁶ or even insulators⁷ has been pursued as well.

Physicists have been attracted in large numbers to these issues because on top of the practical aspects the underlying phenomena are so fascinating. Berger⁸ and Slonczewski⁹ are in general acknowledged to have started the whole field by introducing the concept of current-induced magnetization dynamics by the transfer of spin. The importance of their work was fully appreciated only after experimental confirmation of the predictions in multi-layered structures^{10,11}. The reciprocal effect, *i.e.* the generation of currents by magnetization dynamics now called *spin pumping*, has been expected long ago^{12,13}, but it took some time before Tserkovnyak *et al.*^{14,15} developed a rigorous theory of spin-pumping for magnetic multi-layers, including the associated increased magnetization damping^{16–18}.

B. Discrete versus Homogeneous

Spin-transfer torque and spin pumping in magnetic metallic multi-layers are by now relatively well understood and the topic has been covered by a number of review articles^{15,19,20}. It can be understood very well in terms of a time-dependent extension of magneto-electronic circuit theory^{19,21}, which corresponds to the assumption of spin diffusion in the bulk and quantum mechanical boundary conditions at interfaces. Random matrix theory²² can be shown to be equivalent to circuit theory^{19,23,24}. The technologically important current-induced switching in magnetic tunnel junctions has recently been the focus of attention²⁵. Tunnel junctions limit the transport such that circuit issues are less important, whereas the quantum-mechanical nature of the tunneling process becomes essential. We will not review this issue in more detail here.

The interaction of currents and magnetization in continuous magnetization textures has also attracted much interest, partly due to possible applications such as nonvolatile shift registers²⁶. From a formal point of view the physics of current-magnetization interaction in a continuum poses new challenges as compared to heterostructures with atomically sharp interfaces. In magnetic textures such as magnetic domain walls, currents interact over length scales corresponding to the wall widths that are usually much longer than even the transport mean-free path. Issues of the in-plane *vs.* magnetic-field like torque²⁷ and the spin-motive force in moving magnetization textures²⁸ took some time to get sorted out, but the understanding of the complications associated with continuous textures has matured by now. There is now general consensus about the physics of current-induced magnetization excitations and magnetization dynamics induced currents^{29,30}. Nevertheless, the similarities and differences of spin torque and spin pumping in discrete and continuous magnetic systems has to our knowledge never been discussed in a coherent fashion. It has also only recently been realized that both phenomena are directly related, since they reflect identical microscopic correlations according to the Onsager reciprocity relations^{31–33}.

C. This Chapter

In this Chapter, we (i) review the basic understandings of spin transfer torque *vs.* spin pumping and (ii) knit together our understanding of both concepts for heterogeneous and homogeneous systems. We discuss the general phenomenology guided by Onsager's reciprocity in the linear response regime³⁴. We will compare the in- and out-of-plane spin transfer torques at interfaces as governed by the real and imaginary part of the so-called spin-mixing conductances with that in textures, which are usually associated with the adiabatic torque and its dissipative correction²⁷, usually described by a dimensionless factor β in order to stress the relation with the Gilbert damping constant α . We argue that the spin pumping phenomenon at interfaces between magnets and conductors is identical to the spin-motive force due to magnetization texture dynamics such as moving domain walls²⁸. We emphasize that spin pumping is on a microscopic level identical to the spin transfer torque, thus arriving at a significantly simplified conceptual picture of the coupling between currents and magnetization. We also point out that we are not limited to a phenomenological

description relying on fitting parameters by demonstrating that the material dependence of crucial parameters such as α and β can be computed from first principles.

II. PHENOMENOLOGY

In this Section we explain the basics physics of spin-pumping and spin-transfer torques, introduce the dependence on material and externally applied parameters, and prove their equivalence in terms of Onsager's reciprocity theorem.

A. Mechanics

On a microscopic level electrons behave as wave-like Fermions with quantized intrinsic angular momentum. However, in order to understand the electron wave packets at the Fermi energy in high-density metals and the collective motion of a large number of spins at not too low temperatures classical analogues can be useful.

Spin transfer torque and spin pumping are on a fundamental level mechanical phenomena that can be compared with the game of billiards, which is all about the transfer of linear and angular momenta between the balls and cushions. A skilled player can use the cue to transfer velocity and spin to the billiard ball in a controlled way. The path of the spinning ball is governed by the interaction with the reservoirs of linear and angular momentum (the cushions and the felt/baize) and with other balls during collisions. A ball that for instance hits the cushion at normal angle with top or bottom spin will reverse its rotation and translation, thereby transferring twice its linear and angular moment to the frame of the billiard.

Since the work by Barnett³⁵ and Einstein-de Haas³⁶ almost a century ago, we know that magnetism is caused by the magnetic moment of the electron, which is intimately related with its mechanical angular momentum. How angular momentum transfer occurs between electrons in magnetic structures can be imagined mechanically: just replace the billiard balls by spin polarized electrons and the cushion by a ferromagnet. Good metallic interfaces correspond to a cushion with high friction. The billiard ball reverses angular and linear momentum, whereas the electron is reflected with a spin flip. While the cushion and the billiard table absorb the angular momentum, the magnetization absorbs the spin angular momentum. The absorbed spins correspond to a torque that, if exceeding a critical value, will set the magnetization into motion. Analogously, a time-dependent magnetization injects net angular momentum into a normal metal contact. This "spin pumping" effect, *i.e.* the main topic of this chapter, can be also visualized mechanically: a billiard ball without spin will pick up angular momentum under reflection if the cushion is rotating along its axis.

B. Spin-transfer Torque and Spin-pumping

Ferromagnets do not easily change the modulus of the magnetization vector due to large exchange energy costs. The low-energy excitations, so-called spin waves or magnons, only modulate the magnetization direction with respect to the equilibrium magnetization configuration. In this regime the magnetization dynamics of ferromagnets can be described by the Landau-Lifshitz-Gilbert (LLG) equation,

$$\dot{\mathbf{m}} = -\gamma \mathbf{m} \times \mathbf{H}_{\text{eff}} + \tilde{\alpha} \mathbf{m} \times \dot{\mathbf{m}}, \quad (1)$$

where $\mathbf{m}(\mathbf{r}, t)$ is a unit vector along the magnetization direction, $\dot{\mathbf{m}} = \partial \mathbf{m} / \partial t$, $\gamma = g^* \mu_B / \hbar > 0$ is (minus) the gyro-magnetic ratio in terms of the effective g -factor and the Bohr magneton μ_B , and $\tilde{\alpha}$ is the Gilbert damping tensor that determines the magnetization dissipation rate. Under isothermal conditions the effective magnetic field $\mathbf{H}_{\text{eff}} = -\delta F[\mathbf{m}] / \delta(M_s \mathbf{m})$ is governed by the magnetic free energy F and M_s is the saturation magnetization. We will consider both spatially homogeneous and inhomogeneous situations. In the former case, the magnetization is constant in space (macrospin), while the torques are applied at the interfaces. In the latter case, the effective magnetic field \mathbf{H}_{eff} also includes a second order spatial gradient arising from the (exchange) rigidity of the magnetization and torques as well as motive forces that are distributed in the ferromagnet.

Eq. (1) can be rewritten in the form of the Landau-Lifshitz (LL) equation:

$$(1 + \tilde{\alpha}^2) \dot{\mathbf{m}} = -\gamma \mathbf{m} \times \mathbf{H}_{\text{eff}} - \gamma \tilde{\alpha} \mathbf{m} \times (\mathbf{m} \times \mathbf{H}_{\text{eff}}). \quad (2)$$

Additional torques due to the coupling between currents and magnetization dynamics should be added to the right-hand side of the LLG or LL equation, but some care should be exercised in order to keep track of dissipation in a consistent manner. In our approach the spin-pumping and spin-transfer torque contributions are most naturally

added to the LLG equation (1), but we will also make contact with the LL equation (2) while exploring the Onsager reciprocity relations.

In the remaining part of this section we describe the extensions of the LLG equation due to spin-transfer and spin-pumping torques for discrete and bulk systems in Sec. IIB 1 and Sec. IIB 2, respectively. In the next section we demonstrate in more detail how spin-pumping and spin-transfer torque are related by Onsager reciprocity relations for both discrete and continuous systems.

1. Discrete Systems

Berger and Slonczewski predicted that in spin-valve structures with current perpendicular to the interface planes (CPP) a dc current can excite and even reverse the relative magnetization of magnetic layers separated by a normal metal spacer^{8,9}. The existence of this phenomenon has been amply confirmed by experiments^{10,11,20,37-41}. We can understand current-induced magnetization dynamics from first principles in terms of the coupling of spin-dependent transport with the magnetization. In a ferromagnetic metal majority and minority electron spins have often very different electronic structures. Spins that are polarized non-collinear with respect to the magnetization direction are not eigenstates of the ferromagnet, but can be described as a coherent linear combination of majority and minority electron spins at the given energy shell. If injected at an interface, these states precess on time and length scales that depend on the orbital part of the wave function. In high electron-density transition metal ferromagnets like Co, Ni, and Fe a large number of wave vectors are available at the Fermi energy. A transverse spin current injected from a diffuse reservoir generates a large number of wave functions oscillating with different wave length that lead to efficient destructive interference or decoherence of the spin momentum. Beyond a transverse magnetic coherence length, which in these materials is of the order of the Fermi wave length, typically around 1 nm, a transversely polarized spin current cannot persist.²¹ This destruction of transverse angular momentum is per definition equal to a torque. Slonczewski's spin-transfer torque is therefore equivalent to the absorption of a spin current at an interface between a normal metal and a ferromagnet whose magnetization is transverse to the spin current polarization. Each electron carries an electric charge $-e$ and an angular momentum of $\pm\hbar/2$. The loss of transverse spin angular momentum at the normal metal-ferromagnet interface is therefore $\hbar[\mathbf{I}_s - (\mathbf{I}_s \cdot \mathbf{m})\mathbf{m}]/(2e)$, where the spin-current \mathbf{I}_s is measured in the units of an electrical current, *e.g.* in Ampere. In the macrospin approximation the torque has to be shared with all magnetic moments or $M_s\mathcal{V}$ of the ferromagnetic particle or film with volume \mathcal{V} . The torque on magnetization equals the rate of change of the total magnetic moment of the magnet $\partial(\mathbf{m}M_s\mathcal{V})_{\text{stt}}/\partial t$, which equals the spin current absorption⁹. The rate of change of the magnetization direction therefore reads:

$$\boldsymbol{\tau}_{\text{stt}} = \left(\frac{\partial \mathbf{m}}{\partial t} \right)_{\text{stt}} = -\frac{\gamma \hbar}{2eM_s\mathcal{V}} \mathbf{m} \times (\mathbf{m} \times \mathbf{I}_s). \quad (3)$$

We still need to evaluate the spin current that can be generated, *e.g.*, by the inverse spin Hall effect in the normal metal or optical methods. Here we concentrate on the layered normal metal-ferromagnet systems in which the current generated by an applied bias is polarized by a second highly coercive magnetic layer as in the schematic Fig. 1. Magneto-electronic circuit theory is especially suited to handle such a problem²¹ For simplicity we disregard here

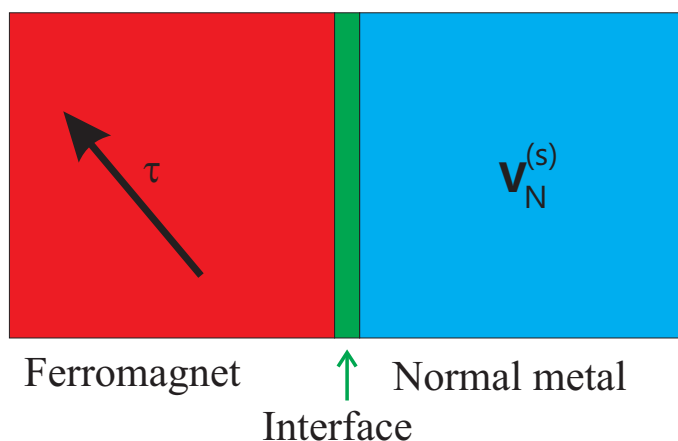


FIG. 1: Illustration of the spin-transfer torque in layered normal metal|ferromagnet system. A spin accumulation $\mathbf{V}_N^{(s)}$ in the normal metal induces a spin-transfer torque $\boldsymbol{\tau}_{\text{stt}}$ on the ferromagnet.

extrinsic dissipation of spin angular momentum due to spin-orbit coupling and disorder, which can be taken into account when the need arises^{42,43}. We allow for a non-equilibrium magnetization or spin accumulation $\mathbf{V}_N^{(s)}$ in the normal metal layer. $\mathbf{V}_N^{(s)}$ is a vector pointing in the direction of the local net magnetization, whose modulus $V_N^{(s)}$ is the difference between the differences in electric potentials (or electrochemical potentials divided by $2e$) of both spin species. Including the charge accumulation $V_N^{(c)}$ (local voltage), the potential experienced by a spin-up (spin-down) electron along the direction of the spin accumulation in the normal metal is $V_N^\uparrow = V_N^{(c)} + V_N^{(s)}$ ($V_N^\downarrow = V_N^{(c)} - V_N^{(s)}$). Inside a ferromagnet, the spin accumulation must be aligned to the magnetization direction $\mathbf{V}_F^{(s)} = \mathbf{m}V_F^{(s)}$. Since $V_F^{(s)}$ does not directly affect the spin-transfer torque at the interface we disregard it for convenience here (see Ref. 19 for a complete treatment), but retain the charge accumulation $V_F^{(c)}$. We can now compute the torque at the interface between a normal metal and a ferromagnet arising from a given spin accumulation $\mathbf{V}_N^{(s)}$. Ohm's Law for the spin-current projections aligned (I_\uparrow) and anti-aligned (I_\downarrow) to the magnetization direction then read^{21,44} (positive currents correspond to charge flowing from the normal metal towards the ferromagnet)

$$I_\uparrow = G_\uparrow \left[\left(V_N^{(c)} - V_F^{(c)} \right) + \mathbf{m} \cdot \left(\mathbf{V}_N^{(s)} - \mathbf{m}V_F^{(c)} \right) \right], \quad (4)$$

$$I_\downarrow = G_\downarrow \left[\left(V_N^{(c)} - V_F^{(c)} \right) - \mathbf{m} \cdot \left(\mathbf{V}_N^{(s)} - \mathbf{m}V_F^{(c)} \right) \right]. \quad (5)$$

where G_\uparrow and G_\downarrow are the spin-dependent interface conductances. The total charge current $I^{(c)} = I_\uparrow + I_\downarrow$, is continuous across the interface, $I_N^{(c)} = I_F^{(c)} = I^{(c)}$. The (longitudinal) spin current defined by Eqs. (4) and (5) $(I_\uparrow - I_\downarrow)\mathbf{m}$ is polarized along the magnetization direction. The transverse part of the spin current can be written as the sum of two vector components in the space spanned by the $\mathbf{m}, \mathbf{V}_N^{(s)}$ plane as well as its normal. The total spin current on the normal metal side close to the interface reads^{19,21}:

$$\mathbf{I}_N^{(s, \text{bias})} = (I_\uparrow - I_\downarrow)\mathbf{m} - 2G_\perp^{(R)}\mathbf{m} \times \left(\mathbf{m} \times \mathbf{V}_N^{(s)} \right) - 2G_\perp^{(I)}\left(\mathbf{m} \times \mathbf{V}_N^{(s)} \right), \quad (6)$$

where $G_\perp^{(R)}$ and $G_\perp^{(I)}$ are two independent transverse interface conductances. $\mathbf{I}_N^{(s, \text{bias})}$ is driven by the external bias $\mathbf{V}_N^{(s)}$ and should be distinguished from the pumped spin current addressed below. (R) and (I) refer to the real and imaginary parts of microscopic expression for these ‘‘spin mixing’’ interface conductances $G_{\uparrow\downarrow}^{(R)} = G_\perp^{(R)} + iG_\perp^{(I)}$.

The transverse components are absorbed in the ferromagnet within a very thin layer. Detailed calculations show that transverse spin-current absorption in the ferromagnet happens within a nanometer from the interface, where disorder suppresses any residual oscillations that survived the above-mentioned destructive interference in ballistic structures⁴⁵. Spin-transfer in transition metal based multilayers is therefore an interface effect, except in ultrathin ferromagnetic films⁴⁶. As discussed above, the divergence of the transverse spin current at the interface gives rise to the torque

$$\boldsymbol{\tau}_{\text{stt}}^{(\text{bias})} = -\frac{\gamma\hbar}{eM_s\mathcal{V}} \left[G_\perp^{(R)}\mathbf{m} \times \left(\mathbf{m} \times \mathbf{V}_N^{(s)} \right) + G_\perp^{(I)}\left(\mathbf{m} \times \mathbf{V}_N^{(s)} \right) \right]. \quad (7)$$

Adding this torque to the Landau-Lifshitz-Gilbert equation leads to the Landau-Lifshitz-Gilbert-Slonczewski (LLGS) equation

$$\dot{\mathbf{m}} = -\gamma\mathbf{m} \times \mathbf{H}_{\text{eff}} + \boldsymbol{\tau}_{\text{stt}}^{(\text{bias})} + \alpha\mathbf{m} \times \dot{\mathbf{m}}. \quad (8)$$

The first term in Eq. (7) is the (Slonczewski) torque in the $(\mathbf{m}, \mathbf{V}_N^{(s)})$ plane, which resembles the Landau-Lifshitz damping in Eq. (2). When the spin-accumulation $\mathbf{V}_N^{(s)}$ is aligned with the effective magnetic field \mathbf{H}_{eff} , the Slonczewski torque effectively enhances the damping of the ferromagnet and stabilizes the magnetization motion towards the equilibrium direction. On the other hand, when $\mathbf{V}_N^{(s)}$ is antiparallel to \mathbf{H}_{eff} , this torque opposes the damping. When exceeding a critical value it leads to precession or reversal of the magnetization. The second term in Eq. (7) proportional to $G_\perp^{(I)}$ modifies the magnetic field torque and precession frequency. While the in-plane torque leads to dissipation of the spin accumulation, the out-of-plane torque induces a precession of the spin accumulation in the ferromagnetic exchange field along \mathbf{m} . It is possible to implement the spin-transfer torque into the Landau-Lifshitz equation, but the conductance parameters differ from those in Eq. (7).

Since spin currents can move magnetizations, it is natural to consider the reciprocal effect, *viz.* the generation of spin currents by magnetization motion. It was recognized in the 1970's that spin dynamics is associated with spin

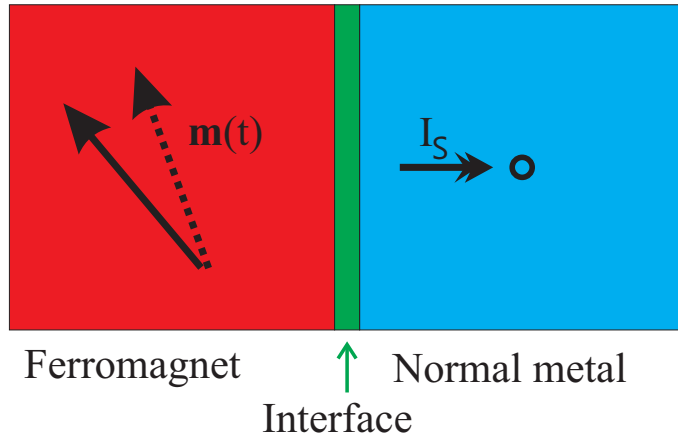


FIG. 2: Spin-pumping in normal metal|ferromagnet systems. A dynamical magnetization “pumps” a spin current $\mathbf{I}^{(s)}$ into an adjacent normal metal.

currents in normal metals. Barnes⁴⁷ studied the dynamics of localized magnetic moments embedded in a conducting medium. He showed that the dynamic susceptibility in diffuse media is limited by the spin-diffusion length. Janossy and Monod¹² and Silsbee *et al.*¹³ postulated a coupling between a dynamic ferromagnetic magnetization and a spin accumulation in adjacent normal metals in order to explain that microwave transmission through normal metal foils is enhanced by a coating with a ferromagnetic layer. The scattering theory for spin currents induced by magnetization dynamics was developed by Tserkovnyak *et al.*¹⁴ on the basis of the theory of adiabatic quantum pumping⁴⁸, hence the name “spin pumping”. Theoretical results were confirmed by the agreement of the spin-pumping induced increase of the Gilbert damping with experiments by Mizukami *et al* and Heinrich *et al.*^{16–18}. A schematic picture of spin-pumping in normal|ferromagnet systems is shown in Fig. 2. At not too high excitations and temperatures, the ferromagnetic dynamics conserves the modulus of the magnetization $M_s \mathbf{m}$. Conservation of angular momentum then implies that the spin current $\mathbf{I}_N^{(s,\text{pump})}$ pumped out of the ferromagnet has to be polarized perpendicularly to \mathbf{m} , *viz.* $\mathbf{m} \cdot \mathbf{I}_N^{(s,\text{pump})} = 0$. Furthermore, the adiabatically pumped spin current is proportional to $|\dot{\mathbf{m}}|$. Under these conditions, therefore,^{14,15}

$$\frac{e}{\hbar} \mathbf{I}_N^{(s,\text{pump})} = G_{\perp}^{\prime(R)} (\mathbf{m} \times \dot{\mathbf{m}}) + G_{\perp}^{\prime(I)} \dot{\mathbf{m}}, \quad (9)$$

where $G_{\perp}^{\prime R}$ and $G_{\perp}^{\prime I}$ are two transverse conductances that depend on the materials. Here the sign is defined to be negative when $\mathbf{I}_N^{(s,\text{pump})}$ implies loss of angular momentum for the ferromagnet. For $|\dot{\mathbf{m}}| \neq 0$, the right-hand side of the LLGS equation (8) must be augmented by Eq. (9). The leakage of angular momentum leads *e.g.* to an enhanced Gilbert damping^{16–18}.

Onsager’s reciprocity relations dictate that conductance parameters in thermodynamically reciprocal processes must be identical when properly normalized. We prove below that spin-transfer torque (7) and spin pumping (9) indeed belong to this category and must be identical, *viz.* $G_{\perp}^{(R)} = G_{\perp}^{\prime(R)}$ and $G_{\perp}^{(I)} = G_{\perp}^{\prime(I)}$. Spin-transfer torque and spin-pumping are therefore opposite sides of the same coin, at least in the linear response regime. Since spin-mixing conductance parameters governing both processes are identical, an accurate measurement of one phenomenon is sufficient to quantify the reciprocal process. Magnetization dynamics induced by the spin-transfer torque are not limited to macrospin excitations and experiments are carried out at high current levels that imply heating and other complications. On the other hand, spin-pumping can be directly detected by the line-width broadening of FMR spectra of thin multilayers. In the absence of two-magnon scattering phenomena and a sufficiently strong static magnetic field, FMR excites only the homogeneous macrospin mode, allowing the measurement of the transverse conductances $G_{\perp}^{\prime(R)}$ and, in principle, $G_{\perp}^{\prime(I)}$. $G_{\perp}^{\prime(I)}$. Experimental results and first-principles calculations^{14,15} agree quantitatively well. Rather than attempting to measure these parameters by current-induced excitation measurements, the values $G_{\perp}^{\prime(R)}$ and $G_{\perp}^{\prime(I)}$ should be inserted, concentrating on other parameters when analyzing these more complex magnetization phenomena. Finally we note that spin mixing conductance parameters can be derived as well from static magnetoresistance measurements in spin valves⁴⁶ or by detecting the spin current directly by the inverse spin Hall effect^{49,50}.

2. Continuous Systems

The coupling effects between (spin-polarized) electrical currents and magnetization dynamics also exist in magnetization textures of bulk metallic ferromagnets. Consider a magnetization that adiabatically varies its direction in space. The dominant contribution to the spin-transfer torque can be identified as a consequence of violation of angular momentum conservation: In a metallic ferromagnet, a charge current is spin polarized along the magnetization direction to leading order in the texture gradients. In the bulk, *i.e.* separated from contacts by more than the spin-diffusion length, the current polarization is $P = (\sigma_{\uparrow} - \sigma_{\downarrow}) / (\sigma_{\uparrow} + \sigma_{\downarrow})$, in terms of the ratio of the conductivities for majority and minority electrons, where we continue to measure spin currents in units of electric currents. We first disregard spin-flip processes that dissipate spin currents to the lattice. To zeroth order in the gradients, the spin current $\mathbf{j}^{(s)}$ flowing in a specified (say x -) direction at position \mathbf{r} is polarized along the local magnetization, $\mathbf{j}^{(s)}(\mathbf{r}) = \mathbf{m}(\mathbf{r})j^{(s)}(\mathbf{r})$. The gradual change of the magnetization direction corresponds to a divergence of the angular momentum of the itinerant electron subsystem, $\partial_x \mathbf{j}^{(s)} = j^{(s)} \partial_x \mathbf{m} + \mathbf{m} \partial_x j^{(s)}$, where the latter term is aligned with the magnetization direction and does not contribute to the magnetization torque. This change of spin current does not leave the electron system but flows into the magnetic order, thus inducing a torque on the magnetization. This process does not cause any dissipation and the torque is reactive, as can be seen as well from its time reversal symmetry. To first order in the texture gradient, or adiabatic limit, and for arbitrary current directions^{51,52}

$$\boldsymbol{\tau}_{\text{stt}}^{(\text{bias})}(\mathbf{r}) = \frac{g^* \mu_B P}{2eM_s} (\mathbf{j} \cdot \nabla) \mathbf{m}, \quad (10)$$

where \mathbf{j} is the charge current density vector and the superscript ‘‘bias’’ indicates that the torque is induced by a voltage bias or electric field. From symmetry arguments another torque should exist that is normal to Eq. (10), but still perpendicular to the magnetization and proportional to the lowest order in its gradient. Such a torque is dissipative, since it changes sign under time reversal. For isotropic systems, we can parameterize the out-of-plane torque by a dimensionless parameter β such that the total torque reads^{27,53},

$$\boldsymbol{\tau}_{\text{stt}}^{(\text{bias})}(\mathbf{r}) = \frac{g^* \mu_B}{2eM_s} \sigma P [(\mathbf{E} \cdot \nabla) \mathbf{m} + \beta \mathbf{m} \times (\mathbf{E} \cdot \nabla) \mathbf{m}], \quad (11)$$

we have used Ohm’s law, $\mathbf{j} = \sigma \mathbf{E}$. In the adiabatic limit, *i.e.* to the first order in the gradient of the magnetization $\partial_i m_j$, the spin-transfer torque Eq. (11) describes how the magnetization dynamics is affected by currents in isotropic ferromagnets.

Analogous to discrete systems, we may expect a process reciprocal to (11) in ferromagnetic textures similar to the spin pumping at interfaces. Since we are now operating in a ferromagnet, a pumped spin current is transformed into a charge current. To leading order a time-dependent texture is expected to pump a current proportional to the rate of change of the magnetization direction and the gradient of the magnetization texture. For isotropic systems, we can express the expected charge current as

$$j_i^{(\text{pump})} = \frac{\hbar}{2e} \sigma P' [\mathbf{m} \times \partial_i \mathbf{m} + \beta' \partial_i \mathbf{m}] \cdot \hat{\mathbf{m}}, \quad (12)$$

where P' is a polarization factor and β' an out-of-plane contribution. Note that we have here been assuming a strong spin-flip rate so that the spin-diffusion length is much smaller than the typical length of the magnetization texture. Volovik considered the opposite limit of weak spin-dissipation and kept track of currents in two independent spin bands⁵¹. In that regime he derived the first term in (12), proportional to P' and proved that $P = P'$. This result was re-derived by Barnes and Maekawa²⁸. The last term, proportional to the β -factor was first discussed by Duine in Ref. (54) for a mean-field model, demonstrating that $\beta = \beta'$. More general textures and spin relaxation regimes were treated by Tserkovnyak and Mecklenburg³¹. In the following we demonstrate by the Onsager reciprocity relations that the coefficients appearing in the spin-transfer torques (11) are identical to those in the pumped current (12), *i.e.* $P = P'$ and $\beta = \beta'$.

The proposed relations for the spin-transfer torques and pumped current in continuous systems form a local relationship between torques, current, and electric and magnetic fields. For ballistic systems, this is not satisfied since the current at one spatial point depends on the electric field in the whole sample or global voltage bias and not just on the local electric field. The local assumption also breaks down in other circumstances. The long-range magnetic dipole interaction typically breaks a ferromagnet into uniform domains. The magnetization gradually changes in the region between the domains, the domain wall. When the domain wall width is smaller than the phase coherence length or the mean free path, one should replace the local approach by a global strategy for magnetization textures in which the dynamics is characterized by one or more dynamic (soft) collective coordinates $\{\xi_a(\tau)\}$ that are allowed to vary (slowly) in time

$$\mathbf{m}(\mathbf{r}\tau) = \mathbf{m}_{\text{st}}(\mathbf{r}; \{\xi_a(\tau)\}), \quad (13)$$

where \mathbf{m}_{st} is a static description of the texture. In order to keep the discussion simple and transparent we disregard thermoelectric effects, which can be important in principle⁵⁵. The thermodynamic forces are $-\partial F/\partial \xi_a$, where F is the free energy as well as the bias voltage across the sample V . In linear response the rate of change of the dynamic collective coordinates and the charge current in the system are related to the thermodynamic forces $-\partial F/\partial \xi$ and V by a response matrix

$$\begin{pmatrix} \dot{\xi} \\ I \end{pmatrix} = \begin{pmatrix} \tilde{L}_{\xi\xi} & \tilde{L}_{\xi I} \\ \tilde{L}_{I\xi} & \tilde{L}_{II} \end{pmatrix} \begin{pmatrix} -\partial F/\partial \xi \\ V \end{pmatrix}, \quad (14)$$

where $\tilde{L}_{\xi V}$ describes the bias voltage-induced torque and $\tilde{L}_{I\xi}$ the current pumped by the moving magnetization texture. These expressions are general and includes *e.g.* effects of spin-orbit interaction. Onsager's reciprocity relations imply $\tilde{L}_{I\xi_i}\{\mathbf{m}, \mathbf{H}\} = \tilde{L}_{\xi_i I}\{-\mathbf{m}, -\mathbf{H}\}$ or $\tilde{L}_{I\xi_i}\{\mathbf{m}, \mathbf{H}\} = \tilde{L}_{\xi_i I}\{-\mathbf{m}, -\mathbf{H}\}$ depending on how the collective coordinates transform under time-reversal. The coefficient $\tilde{L}_{I\xi}$ can be easily expressed in terms of the scattering theory of adiabatic pumping as discussed below. This strategy was employed to demonstrate for (Ga,Mn)As that the spin-orbit interaction can enable a torque arising from a pure charge current bias in Ref. 42 and to compute β in Ref. 32.

3. Self-consistency: Spin-battery and enhanced Gilbert Damping

We discussed two reciprocal effects: torque induced by charge currents (voltage or electric field) on the magnetization and the current induced by a time-dependent magnetization. These two effects are not independent. For instance, in layered systems, when the magnetization precesses, it can pump spins into adjacent normal metal. The spin-pumping affects magnetization dynamics depending on whether the spins return into the ferromagnet or not. When the adjacent normal metal is a good spin sink, this loss of angular momentum affects the magnetization dynamics by an enhanced Gilbert damping. In the opposite limit of little or no spin relaxation in an adjacent conductor of finite size, the pumped steady-state spin-current is canceled by a diffusion spin current arising from the build-up of spin accumulation potential in the adjacent conductor. The build-up of the spin accumulation can be interpreted as a spin battery⁵⁶. Similarly, in magnetization textures, the dynamic magnetization pumps currents that in turn exert a torque on the ferromagnet.

In the spin-battery the total spin-current in the normal metal consists of the diffusion-driven Eq. (6) and the pumped Eq. (9) spin currents⁵⁶. When there are no other intrinsic time-scales in the transport problem (*e.g.* instantaneous diffusion) and in the steady state, conservation of angular momentum dictates that the total spin-current in the normal metal must vanish,

$$\mathbf{I}_N^{(s,\text{bias})} + \mathbf{I}_N^{(s,\text{pump})} = 0,$$

which from Eqs. (6) and (9) results in a spin accumulation, which can be called a spin-battery bias or spin-motive force:

$$e\mathbf{V}_N^{(s)} = \hbar\mathbf{m} \times \dot{\mathbf{m}}. \quad (15)$$

This is a manifestation of Larmor's theorem¹⁵. In diffusive systems, the diffusion of the pumped spins into the normal metal takes a finite amount of time. When the typical diffusion time is longer than the typical precession time, the AC component averages out to zero⁵⁶. In this regime, the spin-battery bias is constant and determined by

$$\left[e\mathbf{V}_N^{(s)} \right]^{(\text{DC})} = \int_{\tau_p} \frac{dt}{\tau_p} \mathbf{m} \times \hbar\dot{\mathbf{m}}, \quad (16)$$

where τ_p is the precession period. Without spin-flip processes, the magnitude of the steady-state spin bias is governed by FMR frequency of the magnetization precession $e\mathbf{V}_N^{(s)} = \hbar\omega_{\text{FMR}}$ and is independent of the interface properties. Spin-flip scattering in the normal metal reduces the spin bias $e\mathbf{V}_N^{(s)} < \hbar\omega_{\text{FMR}}$ in a non-universal way^{15,56}. The loss of spin angular momentum implies a damping torque on the ferromagnet. Asymmetric spin-flip scattering rates in adjacent left and right normal metals can also induced a charge potential difference resulting from the spin-battery, which has been measured.^{57,58} The spin-battery effect has also been measured via the spin Hall effect in Ref.⁵⁹.

In the opposite regime, when spins relax much faster than their typical injection rate into the adjacent normal metal, (3), the net spin-current is well described by the spin-pumping mechanism. According to Eq. (9), in which primes may be removed because of the Onsager reciprocity,

$$\boldsymbol{\tau}_{\text{stt}}^{(\text{pump})} = \frac{\gamma\hbar^2}{2e^2M_s\mathcal{V}} \left[G_{\perp}^{(R)} \mathbf{m} \times \dot{\mathbf{m}} + G_{\perp}^{(I)} \dot{\mathbf{m}} \right]. \quad (17)$$

We use the superscript ‘‘pump’’ to clarify that this torque arises from the emission of spins from the ferromagnet. The first term in Eq. (17) is equal to the Gilbert damping term in the LLG equation (1). This implies that the spin pumping into an adjacent conductor maximally enhances the Gilbert damping by

$$\alpha_{\text{stt}}^{(\text{pump})} = \frac{\gamma \hbar^2}{2e^2 M_s \mathcal{V}} G_{\perp}^{(R)}. \quad (18)$$

This damping is proportional to the interface conductance $G_{\perp}^{(R)}$ and thus the normal metal-ferromagnet surface area as well as inversely proportional to the volume of the ferromagnet and therefore scales as $1/d_F$, where d_F is the thickness of the ferromagnetic layer. The transverse conductance per unit areas agrees well with theory¹⁵. The microscopic expression for $G_{\perp}^{(R)} > 0$ and therefore $\alpha_{\text{stt}}^{(\text{pump})} > 0$. The second term on the right hand side of Eq. (17) in (17), modifies the gyro-magnetic ratio and ω_{FMR} . For conventional ferromagnets like Fe, Ni, and Co, $G_{\perp}^{(I)} \ll G_{\perp}^{(R)}$ by near cancellation of positive and negative contributions in momentum space. In these systems $G_{\perp}^{(I)}$ is much smaller than $G_{\perp}^{(R)}$ and the effects of $G_{\perp}^{(I)}$ might therefore be difficult to observe.

A similar argument leads us to expect an enhancement of the Gilbert damping in magnetic textures. By inserting the pumped current Eq. (12) into the torque Eq. (11) in place of $\sigma \mathbf{E}$, we find a contribution caused by the magnetization dynamics^{60–62}

$$\boldsymbol{\tau}_{\text{stt}}^{(\text{drift})}(\mathbf{r}) = \frac{\gamma \hbar^2}{4e^2 M_s} P^2 \sigma [([\mathbf{m} \times \partial_i \mathbf{m} + \beta \partial_i \mathbf{m}] \cdot \dot{\mathbf{m}}) + \beta \mathbf{m} \times ([\mathbf{m} \times \partial_i \mathbf{m} + \beta \partial_i \mathbf{m}] \cdot \dot{\mathbf{m}}_i)] \partial_i \mathbf{m}, \quad (19)$$

which gives rise to additional dissipation of the order $\gamma \hbar^2 P^2 \sigma / 4e^2 M_s \lambda_w^2$, where λ_w is the typical length scale for the variation of the magnetization texture such as the domain wall width or the radius of a vortex. Eq. (19) inserted into the LLG equation also renormalizes the gyromagnetic ratio by an additional factor β . The additional dissipation becomes important for large gradients as in narrow domain walls and close to magnetic vortex centers^{60,62}.

Finally, we point out that the fluctuation-dissipation theorem dictates that equilibrium spin-current fluctuations associated with spin-pumping by thermal fluctuations must lead to magnetization dissipation. This connection was worked out in Ref. 63.

C. Onsager Reciprocity Relations

The Onsager reciprocity relations express fundamental symmetries in the linear response matrix relating thermodynamic forces and currents. In normal metal/ferromagnetic heterostructures, a spin accumulation in the normal metal in contact with a ferromagnet can exert a torque on the ferromagnet, see Eq. (7). The reciprocal process is spin pumping, a precessing ferromagnet induces a spin current in the adjacent normal metal as described by Eq. (9). Both these effects are non-local since the spin-transfer torque on the ferromagnet arises from the spin accumulation potential in the normal metal and the pumped spin current in the normal metal is a result of the collective magnetization dynamics. In bulk ferromagnets, a current (or electric field) induces a spin-transfer torque on a magnetization texture. The reciprocal pumping effect is now an electric current (or emf) generated by the texture dynamics. In the next two subsections we provide technical details of the derivation of the Onsager reciprocity relations under these circumstance

1. Discrete Systems

As an example of a discrete system, we consider a normal metal-ferromagnet bilayer without any spin-orbit interaction (see Ref. 42 for a more general treatment that takes spin-flip processes into account) and under isothermal conditions (the effects of temperature gradients are discussed in Refs. 33,64,65). The spin-transfer physics is induced by a pure spin accumulation in the normal metal, whose creation does not concern us here. The central ingredients for the Onsager’s reciprocity relations are the thermodynamic variables with associated forces and currents that are related by a linear response matrix³⁴. In order to uniquely define the linear response, currents J and forces X have to be normalized such that $\dot{F} = \sum XJ$. This is conventionally done by the rate of change of the free energy in the non-equilibrium situation in terms of currents and forces³⁴.

Let us consider first the electronic degrees of freedom. In the normal metal reservoir of a constant spin accumulation $\mathbf{V}_N^{(s)}$ the rate of change of the free energy F_N in terms of the total spin \mathbf{s}_N (in units of electric charge e) reads

$$\dot{F}_N = -\dot{\mathbf{s}}_N \cdot \mathbf{V}_N^{(s)}. \quad (20)$$

This identifies $\mathbf{V}_N^{(s)}$ as a thermodynamic force that induces spin currents $\mathbf{I}_s = \dot{\mathbf{s}}_N$, which is defined to be positive when leaving the normal metal. In the ferromagnet, all spins are aligned along the magnetization direction \mathbf{m} . The associated spin accumulation potential $V_F^{(s)}$ can only induce a contribution to the longitudinal part of the spin current, *e.g.* a contribution to the spin-current along the magnetization direction \mathbf{m} . In our discussion of the Onsager reciprocity relations, we will set this potential to zero for simplicity and disregard associated change in the free energy, but it is straightforward to include the effects of a finite $V_F^{(s)}$.¹⁹

Next, we address the rate of change of the free energy related to the magnetic degrees of freedom in the ferromagnet,

$$\dot{F}(\mathbf{m}) = -M_s \mathcal{V} \mathbf{H}_{\text{eff}} \cdot \dot{\mathbf{m}}/T,$$

where $F(\mathbf{m})$ is the magnetic free energy. The total magnetic moment $M_s \mathcal{V} \mathbf{m}$ is a thermodynamic quantity and the effective magnetic field $\mathbf{H}_{\text{eff}} = -\partial F / \partial (M_s \mathcal{V} \mathbf{m})$ is the thermodynamic force that drives the magnetization dynamics $\dot{\mathbf{m}}$.

In linear response, the spin current $\mathbf{I}_s = \dot{\mathbf{s}}$ and magnetization dynamics $M_s \mathcal{V} \dot{\mathbf{m}}$ are related to the thermodynamic forces as

$$\begin{pmatrix} M_s \mathcal{V} \dot{\mathbf{m}} \\ \mathbf{I}_N^{(s)} \end{pmatrix} = \begin{pmatrix} \tilde{L}^{(mm)} & \tilde{L}^{(ms)} \\ \tilde{L}^{(sm)} & \tilde{L}^{(ss)} \end{pmatrix} \begin{pmatrix} \mathbf{H}_{\text{eff}} \\ \mathbf{V}_N^{(s)} \end{pmatrix}, \quad (21)$$

where $\tilde{L}^{(mm)}$, $\tilde{L}^{(ms)}$, $\tilde{L}^{(sm)}$, and $\tilde{L}^{(ss)}$ are 3×3 tensors in, *e.g.*, a Cartesian basis for the spin and magnetic moment vectors. Onsager discovered that microscopic time-reversal symmetry leads to relations between the off-diagonal components of these linear-response coefficients. Both magnetization in the ferromagnet and the spin-accumulation in the normal metal are anti-symmetric under time-reversal leading to the reciprocity relations

$$L_{ij}^{(sm)}(\mathbf{m}) = L_{ji}^{(ms)}(-\mathbf{m}). \quad (22)$$

Some care should be taken when identifying the Onsager symmetries in spin accumulation-induced magnetization dynamics. Specifically, the LLGS equation (8) cannot simply be combined with the linear response relation (21) and Eq. (22). Only the Landau-Lifshitz-Slonczewski (LL) Eq. (2) directly relates $\dot{\mathbf{m}}$ to \mathbf{H}_{eff} as required by Eq. (21). In terms of the 3×3 matrix \tilde{O} *e.g.*

$$\tilde{O}_{ij}(\mathbf{m}) = \sum_k \epsilon_{ikj} m_k, \quad (23)$$

where $\epsilon_{ijk} = \frac{1}{2} (j - i) (k - i) (k - j)$ is the Levi-Civita tensor, $\mathbf{m} \times \mathbf{H}_{\text{eff}} = \tilde{O} \mathbf{H}_{\text{eff}}$, and the LLGS (8) equation can be written as

$$\left(1 - \alpha \tilde{O}\right) \dot{\mathbf{m}} = \tilde{O} (-\gamma \mathbf{H}_{\text{eff}}) + \boldsymbol{\tau}_{\text{stt}}. \quad (24)$$

By Eq. (21), the pumped current in the absence of a spin accumulation ($\mathbf{V}_N^{(s)} = 0$) is $\mathbf{I}_N^{(s)} = \tilde{L}^{(sm)} \mathbf{H}_{\text{eff}}$. Then, by Eq. (9), $\mathbf{I}_N^{(s)} = \tilde{X}^{(sm)} \dot{\mathbf{m}}$, where the 3×3 tensor $\tilde{X}^{(sm)}$ has components

$$\tilde{X}_{ij}^{(sm)}(\mathbf{m}) = -\frac{\hbar}{e} \left[G_{\perp}^{(R)} \sum_n \epsilon_{inj} m_n + G_{\perp}^{(I)} \sum_{nkl} \epsilon_{ink} m_n \epsilon_{klj} m_k \right]. \quad (25)$$

From the LLG equation (24) for a vanishing spin accumulation ($\mathbf{V}_N^{(s)} = 0$) and thus no bias-induced spin-transfer torque ($\boldsymbol{\tau}_{\text{stt}}^{(\text{bias})} = 0$), the pumped spin current can be expressed as $\mathbf{I}_N^{(s)} = \tilde{X}^{(sm)} \tilde{O} [1 - \alpha \tilde{O}]^{-1} (-\gamma \mathbf{H}_{\text{eff}})$, which identifies the linear response coefficient $\tilde{L}^{(sm)}$ in terms of $\tilde{X}^{(sm)}$ as

$$\tilde{L}^{(sm)} = -\gamma \tilde{X}^{(sm)} \tilde{O} [1 - \alpha \tilde{O}]^{-1}. \quad (26)$$

Using the Onsager relation (22) and noticing that $\tilde{O}_{ij}(\mathbf{m}) = \tilde{O}_{ji}(-\mathbf{m})$ and $\tilde{X}_{ij}^{(sm)}(\mathbf{m}) = \tilde{X}_{ji}^{(sm)}(-\mathbf{m})$

$$\tilde{L}^{(ms)} = -\gamma [1 - \alpha \tilde{O}]^{-1} \tilde{O} \tilde{X}^{(sm)}. \quad (27)$$

The rate of change of the magnetization by the spin accumulation therefore becomes

$$\begin{aligned}\dot{\mathbf{m}}_{\text{stt}} &= \frac{1}{M_s \mathcal{V}} \tilde{L}^{(ms)} \mathbf{V}_N^{(s)}, \\ &= -\frac{\gamma}{M_s \mathcal{V}} \left[1 - \alpha \tilde{O}\right]^{-1} \tilde{O} X^{(sm)} \mathbf{V}_N^{(s)}.\end{aligned}\quad (28)$$

Furthermore, the LLGS equation (24) in the absence of an external magnetic field reads $\left[1 - \alpha \tilde{O}\right] \dot{\mathbf{m}}_{\text{stt}} = \boldsymbol{\tau}_{\text{stt}}^{(\text{drift})}$. Inserting the phenomenological expression for the spin-transfer torque (7), we identify the linear response coefficient $\tilde{L}^{(ms)}$:

$$\begin{aligned}\boldsymbol{\tau}_{\text{stt}}^{(\text{drift})} &= -\frac{\gamma}{M_s \mathcal{V}} \tilde{O} X^{(sm)} \mathbf{V}_N^{(s)}. \\ &= \frac{\gamma}{M_s \mathcal{V} e} \left[G_{\perp}^{\prime(R)} \mathbf{m} \times \left(\mathbf{m} \times \mathbf{V}_N^{(s)} \right) + G_{\perp}^{\prime(I)} \left(\mathbf{m} \times \mathbf{V}_N^{(s)} \right) \right].\end{aligned}\quad (29)$$

This agrees with the phenomenological expression (7) when

$$G_{\perp}^{\prime(R)} = G_{\perp}^{(R)}; \quad G_{\perp}^{\prime(I)} = G_{\perp}^{(I)}.\quad (30)$$

Spin-pumping as expressed by Eq. (9) is thus reciprocal to the spin-transfer torque as described by Eq. (7). In Sec.III A 1 these relations are derived by first principles from quantum mechanical scattering theory, resulting in $G_{\perp}^{\prime(R)} = G_{\uparrow\downarrow} = (e^2/h) \sum_{nm} \left[\delta_{nm} - r_{nm}^{\uparrow} (r_{nm}^{\downarrow})^* \right]$ for a narrow constriction, where r_{nm}^{\uparrow} (r_{nm}^{\downarrow}) is the reflection coefficient for spin-up (spin-down) electrons from waveguide m to waveguide mode n . For layered systems with a constant cross section the microscopic expressions of the transverse (mixing) conductances should be renormalized by taking into account the contributions from the Sharvin resistances^{23,66}, which increases the conductance by roughly a factor of two and is important for a quantitatively comparison between theory and experiments.^{15,19}

2. Continuous Systems

The Onsager reciprocity relations also relate the magnetization torques and currents in the magnetization texture of bulk magnets. Following Refs. (31,32), the rate of change of the free energy related to the electronic freedom in the ferromagnet is $\dot{F}_F = -\int d\mathbf{r} \dot{q} V$, where q is the charge density and $eV = \mu$ is the chemical potential. Inserting charge conservation, $\dot{q} + \nabla \cdot \mathbf{j} = 0$ and by partial integration

$$\dot{F}_F = -\int d\mathbf{r} \mathbf{j} \cdot \mathbf{E}\quad (31)$$

which identifies charge as a thermodynamic variable, while the electric field $\mathbf{E} = \nabla V$ is a thermodynamic force which drives the current density \mathbf{j} . For the magnetic degrees of freedom, the rate of change of the free energy (or entropy) is

$$\dot{F}_m = -M_s \int d\mathbf{r} \dot{\mathbf{m}}(\mathbf{r}) \cdot \mathbf{H}_{\text{eff}}(\mathbf{r}).\quad (32)$$

Just like for discrete systems, $\mathbf{H}_{\text{eff}}(\mathbf{r})$, is the thermodynamic force and $M_s \mathbf{m}$ is the thermodynamic variable to which it couples. In a local approximation the (linear) response depends only on the force at the same location:

$$\begin{pmatrix} M_s \dot{\mathbf{m}} \\ \mathbf{j} \end{pmatrix} = \begin{pmatrix} \tilde{L}^{(mm)} & \tilde{L}^{(mE)} \\ \tilde{L}^{(Em)} & \tilde{L}^{(EE)} \end{pmatrix} \begin{pmatrix} M_s \mathbf{H}_{\text{eff}} \\ \mathbf{E} \end{pmatrix},\quad (33)$$

where $\tilde{L}^{(mm)}$, $\tilde{L}^{(mj)}$, $\tilde{L}^{(jm)}$, and $\tilde{L}^{(jj)}$ are the local response functions. Onsager's reciprocity relations dictate again that

$$\tilde{L}_{ji}^{(jm)}(\mathbf{m}) = \tilde{L}_{ij}^{(mj)}(-\mathbf{m}).\quad (34)$$

Starting from the expression for current pumping (12), we can determine the linear response coefficient $\tilde{L}^{(Em)}$ from

$$\left[\tilde{L}^{(Em)} \left[1 - \alpha \tilde{O} \right] \tilde{O}^{-1} \right]_{ij} = -\gamma \frac{\hbar}{2e} \sigma P' \left[\epsilon_{jkl} m_k \partial_i m_l + \beta' \partial_i m_j \right],\quad (35)$$



FIG. 3: Schematic of how transport between a normal metal and a ferromagnet is computed by scattering theory. The scattering region, which may contain the normal metal-ferromagnet interface and diffusive parts of the normal metal as well as ferromagnet, is attached to real or fictitious leads that are in contact with a left and right reservoir. In the reservoirs, the distributions of charges and spins are assumed to be known via the charge potential and spin accumulation bias.

where the operator \tilde{O} is introduced in the same way as for discrete systems (23) to transform the LLG equation into the LL form (24). According to Eq. (34)

$$\left[\tilde{O}^{-1} \left[1 - \alpha \tilde{O} \right] \tilde{L}^{(mj)} \right]_{ij} = -\gamma \frac{\hbar}{2e} \sigma P' [\epsilon_{ikl} m_k \partial_j m_l - \beta' \partial_j m_i]. \quad (36)$$

The change in the magnetization induced by an electric field is then $M_s \dot{\mathbf{m}}_{\text{stt}}^{(\text{bias})} = \tilde{L}^{(mj)} \mathbf{E}$ so that the spin-transfer torque due to a drift current $\boldsymbol{\tau}_{\text{stt}}^{(\text{bias})} = \left[1 - \alpha \tilde{O} \right] \dot{\mathbf{m}}_{\text{stt}}^{(\text{bias})}$ can be written as

$$\boldsymbol{\tau}_{\text{stt}}^{(\text{bias})} = -\frac{\gamma \hbar}{2e M_s} \sigma P' \epsilon_{imn} m_m [\epsilon_{nkl} m_k E_j \partial_j m_l - \beta' E_j \partial_j m_n] \quad (37)$$

$$\boldsymbol{\tau}_{\text{stt}}^{(\text{bias})} = \gamma \frac{g^* \mu_B}{2e M_s} \sigma P' [(\mathbf{E} \cdot \nabla) \mathbf{m} + \beta' \mathbf{m} \times \mathbf{E} \cdot \nabla \mathbf{m}]. \quad (38)$$

This result agrees with the phenomenological expression for the pumped current (12) when $P = P'$ and $\beta = \beta'$. Therefore, the pumped current and the spin-transfer torque in continuous systems are reciprocal processes. The pumped current can be formulated as the response to a spin-motive force²⁸.

In small systems and thin wires, the current-voltage relation is not well represented by a local approximation. A global approach based on collective coordinates as outlined around Eq. (13) is then a good choice to keep the computational effort in check. Of course, the Onsager reciprocity relations between the pumped current and the effective current-induced torques on the magnetization hold then as well³².

III. MICROSCOPIC DERIVATIONS

A. Spin-transfer Torque

1. Discrete Systems - Magneto-electronic Circuit Theory

Physical properties across a scattering region can be expressed in terms of the region's scattering matrix, which requires a separation of the system into reservoirs, leads, and a scattering region, see Fig. (3). In the lead with index α , the field operator for spin s -electrons is⁶⁷

$$\hat{\Psi}_\alpha^{(s)} = \int \frac{d\epsilon}{\sqrt{2\pi}} \left[v_\alpha^{(ns)} \right]^{-1/2} \sum_{n\sigma} \varphi_\alpha^{(ns)}(\boldsymbol{\rho}) e^{-i\epsilon_\alpha^{(nks)} t / \hbar} \left[e^{ikx} \hat{a}_\alpha^{(ns)}(\epsilon) + e^{-ikx} \hat{b}_\alpha^{(ns)}(\epsilon) \right] \quad (39)$$

in terms of the annihilation operators $\hat{a}_\alpha^{(ns)}$ ($\hat{b}_\alpha^{(ns)}$) for particles incident on (outgoing from) the scattering region in transverse wave guide modes with orbital quantum number n and spin quantum number s ($s = \uparrow$ or $s = \downarrow$). Furthermore, the transverse wave function is $\varphi_\alpha^{(ns)}(\boldsymbol{\rho})$, the transverse coordinate $\boldsymbol{\rho}$, the longitudinal coordinate along the waveguide is x and $v_\alpha^{(ns)}$ is the longitudinal velocity for waveguide mode ns . The positive definite momentum k is related to the energy ϵ by $\hbar k = (2m\epsilon)^{1/2}$. The annihilation operators for incident and outgoing electrons are related by the scattering matrix

$$\hat{b}_\alpha^{(ns)}(\epsilon) = \sum_{\beta m s'} S_{\alpha\beta}^{(nsm s')}(\epsilon) \hat{a}_\beta^{(ms')}(\epsilon). \quad (40)$$

In the basis of the leads ($\alpha = N$ (normal metal) or $\alpha = F$ (ferromagnet)), the scattering matrix is

$$S = \begin{pmatrix} r & t \\ t' & r' \end{pmatrix},$$

where r (t) is a matrix of the reflection (transmission) coefficients between the wave guide modes for an electron incident from the left. Similarly, r' and t' characterize processes where the electron is incident from the right.

In terms of the field operators defined by Eq. (39) and the scattering matrix Eq. (40), at low frequencies, the spin current that flows in the normal metal $\alpha = N$ in the direction towards the scattering region is

$$\mathbf{I}_\alpha^{(s)}(t) = \frac{e}{\hbar} \int_{-\infty}^{\infty} d\epsilon_1 \int_{-\infty}^{\infty} d\epsilon_2 \sum_{\beta\gamma} \sum_{nml} \sum_{\sigma\sigma'} \exp(i(\epsilon_1 - \epsilon_2)t/\hbar) \mathbf{A}_{\alpha\beta, \alpha\gamma}^{(nm, nl), (\sigma, \sigma')}(\epsilon_1, \epsilon_2) \hat{a}_\beta^{(m\sigma)\dagger}(\epsilon_1) \hat{a}_\gamma^{(l\sigma')}(\epsilon_2), \quad (41)$$

where

$$\mathbf{A}_{\alpha\beta, \alpha\gamma}^{(nm, nl), (\sigma, \sigma')}(\epsilon_1, \epsilon_2) = \sum_{ss'} \left[\delta_{\alpha\beta} \delta^{(nm)} \delta^{(s\sigma)} \delta_{\alpha\gamma} \delta^{(nl)} \delta^{(s'\sigma')} - S_{\alpha\beta}^{(ns, m\sigma)*}(\epsilon_1) S_{\alpha\gamma}^{(ns', l\sigma')}(\epsilon_2) \right] \boldsymbol{\sigma}^{(ss')}$$

and $\boldsymbol{\sigma}^{(ss')}$ is a vector of the 2×2 Pauli matrices that depends on the spin indices s and s' of the waveguide mode. The charge current can be found in a similar way. We are interested in the expectation value of the spin-current (41) when the system is driven out-of-equilibrium. In *equilibrium*, the expectation values are

$$\left\langle \hat{a}_\alpha^{(ns)\dagger}(\epsilon) \hat{a}_\beta^{(ms')}(\epsilon') \right\rangle_{\text{eq}} = \delta(\epsilon - \epsilon') \delta_{\alpha\beta} \delta^{(ss')} \delta^{(nm)} f_{\text{FD}}(\epsilon), \quad (42)$$

where $f_{\text{FD}}(\epsilon)$ is the Fermi-Dirac distribution of electrons with energy ϵ . A non-equilibrium spin-accumulation in the normal metal reservoir is not captured by the local equilibrium ansatz in Eq. (42), however. A spin accumulation in the normal metal reservoir can still be postulated when spin-flip dissipation is slow compared to all other relevant time scales. We assume the normal metal and ferromagnet have an isotropic distribution of spins in the orbital space, and for clarity consider no charge bias. The expectation for the number of charges and spins in the waveguide describing normal metal leads attached to the normal reservoirs are

$$\left\langle \hat{a}_N^{(ns)\dagger}(\epsilon) \hat{a}_N^{(ms')}(\epsilon') \right\rangle = \delta(\epsilon - \epsilon') \left[\delta^{(mn)} \delta^{(ss')} f_{\text{FD}}(\epsilon) + \delta^{(mn)} f_N^{(s's)}(\epsilon) \right]. \quad (43)$$

The spin-accumulation $\mathbf{V}_N^{(s)}$ is related to the 2×2 out-of-equilibrium distribution matrix $f_N^{(s's)}(\epsilon)$ by

$$\boldsymbol{\sigma}^{(ss')} \cdot \mathbf{V}_N^{(s)} = \int_{-\infty}^{\infty} d\epsilon f_N^{(s's)}(\epsilon)/e. \quad (44)$$

For the spin-transfer physics, a bias voltage in the ferromagnet does not contribute since it only gives rise to a charge current and a longitudinal spin current. As in the previous section, we therefore set this voltage to zero for simplicity, so that in the ferromagnetic lead attached to the ferromagnetic reservoir

$$\left\langle \hat{a}_F^{(ns)\dagger}(\epsilon) \hat{a}_F^{(ms')}(\epsilon') \right\rangle = \delta(\epsilon - \epsilon') \delta^{(ms)} \delta^{(s's)} f_{\text{FD}}(\epsilon). \quad (45)$$

Furthermore, the expectation values of the cross-correlations remain zero also out-of-equilibrium, $\left\langle \hat{a}_N^{(ns)\dagger}(\epsilon) \hat{a}_F^{(ms')}(\epsilon') \right\rangle = 0$. The spin current in lead α is then

$$\mathbf{I}_\alpha^{(s)}(t) = \frac{e}{\hbar} \int_{-\infty}^{\infty} d\epsilon \sum_{nml} \sum_{ss'\sigma\sigma'} \left[\delta^{(nm)} \delta^{(s\sigma)} \delta^{(nl)} \delta^{(s'\sigma')} - r_{NN}^{(ns, m\sigma)*} r_{NN}^{(ns', l\sigma')} \right] \boldsymbol{\sigma}^{(\sigma\sigma')} f(\sigma'\sigma). \quad (46)$$

Without spin-flip scattering, the reflection coefficient can be expressed as

$$r_{NN}^{nsm\sigma} = \left(r_{NN}^{nm, \uparrow} + r_{NN}^{nm, \downarrow} \right) \delta^{(s\sigma)} / 2 + \mathbf{m} \cdot \boldsymbol{\sigma}_{s\sigma} \left(r_{NN}^{nm, \uparrow} - r_{NN}^{nm, \downarrow} \right) / 2 \quad (47)$$

which can be represented in spin space as

$$r_{NN}^{nsm\sigma} = r_{NN}^{nm, (c)} 1 + r_{NN}^{nm, (s)} \mathbf{m} \cdot \boldsymbol{\sigma} \quad (48)$$

since the scattering matrix can be decomposed into components aligned and anti-aligned with the magnetization direction. These matrices only depend on the orbital quantum numbers (n and m). Using the representation of the out-of-equilibrium spin density in terms of the spin accumulation (44)²¹,

$$\mathbf{I}_N^{(s)} = (G_\uparrow + G_\downarrow) \mathbf{m} \left(\mathbf{m} \cdot \mathbf{V}_N^{(s)} \right) - 2G_\perp^{(R)} \mathbf{m} \times \left(\mathbf{m} \times \mathbf{V}_N^{(s)} \right) - 2G_\perp^{(I)} \left(\mathbf{m} \times \mathbf{V}_N^{(s)} \right) \quad (49)$$

in agreement with (6) when there is no bias voltage in the ferromagnet ($V_F = 0$) which we have assumed for clarity here. We identify the microscopic expressions for the conductances²¹ associated with spins aligned and anti-aligned with the magnetization direction

$$G_\uparrow = \frac{e^2}{h} \sum_{nm} \left[\delta_{nm} - \left| r_{NN}^{nm,\uparrow} \right|^2 \right], \quad (50)$$

$$G_\downarrow = \frac{e^2}{h} \sum_{nm} \left[\delta_{nm} - \left| r_{NN}^{nm,\downarrow} \right|^2 \right], \quad (51)$$

and the transverse (complex valued) spin-mixing conductance

$$G_\perp = \frac{e^2}{h} \sum_{nm} \left[\delta_{nm} - r_{NN}^{nm,\uparrow} r_{NN}^{nm,\downarrow*} \right]. \quad (52)$$

These results are valid when the transmission coefficients are small such that currents do not affect the reservoirs. Otherwise, the transverse conductance parameters should be renormalized by taking into account the Sharvin resistances, as described above^{23,66}. In the limit we considered here, the expression for the spin-current depends only on the reflection coefficients for transport from the normal metal towards the ferromagnet and not on the transmission coefficients for propagation from the normal metal into the ferromagnet. This follows from our assumption that the ferromagnet is longer than the transverse coherence length as well as our disregard of the spin accumulation in the ferromagnet. Both assumptions can be easily relaxed if necessary^{15,19}.

2. Continuous Systems

Spin torques in continuous spin textures can be studied by either quantum kinetic theory,⁶⁸ imaginary-time⁶⁹ and functional Keldysh⁷⁰ diagrammatic approaches, or the scattering-matrix formalism.³² The latter is particularly powerful when dealing with nontrivial band structures with strong spin-orbit interactions, while the others give complementary insight, but are mostly limited to simple model studies. When the magnetic texture is sufficiently smooth on the relevant length scales (the transverse spin coherence length and, in special cases, the spin-orbit precession length) the spin torque can be expanded in terms of the local magnetization and current density as well as their spatial-temporal derivatives. An example is the phenomenological Eq. (11) for the electric-field driven magnetization dynamics of an isotropic ferromagnet. While the physical meaning of the coefficients is clear, the microscopic origin and magnitude of the dimensionless parameter β has still to be clarified.

The solution of the LLG equation (1) appended by these spin torques depends sensitively on the relationship between the dimensionless Gilbert damping constant α and the dissipative spin-torque parameter β : the special case $\beta/\alpha = 1$ effectively manifests Galilean invariance⁷¹ while the limits $\beta/\alpha \gg 1$ and $\beta/\alpha \ll 1$ are regimes of qualitatively distinct macroscopic behavior. The ratio β/α determines the onset of the ferromagnetic current-driven instability⁶⁸ as well as the Walker threshold⁷² for the current-driven domain-wall motion⁵³, and both diverge as $\beta/\alpha \rightarrow 1$. The sub-threshold current-driven domain-wall velocity is proportional to β/α ,²⁷ while $\beta/\alpha = 1$ is a special point, at which the effect of a uniform current density \mathbf{j} on the magnetization dynamics is eliminated in the frame of reference that moves with velocity $\mathbf{v} \propto \mathbf{j}$, which is of the order of the electron drift velocity.⁷³ Although the exact ratio β/α is a system-dependent quantity, some qualitative aspects not too sensitive to the microscopic origin of these parameters have been discussed in relation to metallic systems.^{68,69,71,74} However, these approaches fail for strongly spin-orbit coupled systems such as dilute magnetic semiconductors³².

Let us outline the microscopic origin of β for a simple toy model for a ferromagnet. In Ref. 68, we developed a self-consistent mean-field approach, in which itinerant electrons are described by a single-particle Hamiltonian

$$\hat{\mathcal{H}} = [\mathcal{H}_0 + U(\mathbf{r}, t)] \hat{1} + \frac{\gamma \hbar}{2} \hat{\boldsymbol{\sigma}} \cdot (\mathbf{H} + \mathbf{H}_{\text{xc}})(\mathbf{r}, t) + \hat{\mathcal{H}}_\sigma, \quad (53)$$

where the unit matrix $\hat{1}$ and a vector of Pauli matrices $\hat{\boldsymbol{\sigma}} = (\hat{\sigma}_x, \hat{\sigma}_y, \hat{\sigma}_z)$ form a basis for the Hamiltonian in spin space. \mathcal{H}_0 is the crystal Hamiltonian including kinetic and potential energy. U is the scalar potential consisting of

disorder and applied electric-field contributions. The total magnetic field consists of the applied, \mathbf{H} , and exchange, \mathbf{H}_{xc} , fields that, like U , are parametrically time dependent. Finally, the last term in the Hamiltonian, $\hat{\mathcal{H}}_{\sigma}$, accounts for spin-dephasing processes, *e.g.* due to quenched magnetic disorder or spin-orbit scattering associated with impurity potentials. This last term is responsible for low-frequency dissipative processes affecting dimensionless parameters α and β in the collective equation of motion.

In the time-dependent spin-density-functional theory^{75–77} of itinerant ferromagnetism, the exchange field \mathbf{H}_{xc} is a functional of the time-dependent spin-density matrix

$$\rho_{\alpha\beta}(\mathbf{r}, t) = \langle \hat{\Psi}_{\beta}^{\dagger}(\mathbf{r}) \hat{\Psi}_{\alpha}(\mathbf{r}) \rangle_t, \quad (54)$$

where $\hat{\Psi}$'s are electronic field operators, which should be computed self-consistently as solutions of the Schrödinger equation for $\hat{\mathcal{H}}$. The spin density of conducting electrons is given by

$$\mathbf{s}(\mathbf{r}) = \frac{\hbar}{2} \text{Tr} [\hat{\boldsymbol{\sigma}} \hat{\rho}(\mathbf{r})]. \quad (55)$$

We focus on low-energy magnetic fluctuations that are long ranged and transverse and restrict our attention to a single parabolic band. Consideration of more realistic band structures is also in principle possible from this starting point⁷⁸. We adopt the adiabatic local-density approximation (ALDA, essentially the Stoner model) for the exchange field:

$$\gamma \hbar \mathbf{H}_{\text{xc}}[\hat{\rho}](\mathbf{r}, t) \approx \Delta_{\text{xc}} \mathbf{m}(\mathbf{r}, t), \quad (56)$$

with direction $\mathbf{m} = -\mathbf{s}/s$ locked to the time-dependent spin density (55).

In another simple model of ferromagnetism, the so-called *s-d* model, conducting *s* electrons interact with the exchange field of the *d* electrons that are assumed to be localized to the crystal lattice sites. The *d*-orbital electron spins account for most of the magnetic moment. Because *d*-electron shells have large net spins and strong ferromagnetic correlations, they are usually treated classically. In a mean-field *s-d* description, therefore, conducting *s* orbitals are described by the same Hamiltonian (53) with an exchange field (56). The differences between the Stoner and *s-d* models for the magnetization dynamics are subtle and rather minor. In the ALDA/Stoner model, the exchange potential is (on the scale of the magnetization dynamics) instantaneously aligned with the total magnetization. In contrast, the direction of the unit vector \mathbf{m} in the *s-d* model corresponds to the *d* magnetization, which is allowed to be slightly misaligned with the *s* magnetization, transferring angular momentum between the *s* and *d* magnetic moments. Since most of the magnetization is carried by the latter, the external field \mathbf{H} couples mainly to the *d* spins, while the *s* spins respond to and follow the time-dependent exchange field (56). As Δ_{xc} is usually much larger than the external (including demagnetization and anisotropy) fields that drive collective magnetization dynamics, the total magnetic moment will always be very close to \mathbf{m} . A more important difference of the philosophy behind the two models is the presumed shielding of the *d* orbitals from external disorder. The reduced coupling with dissipative degrees of freedom would imply that their dynamics are more coherent. Consequently, the magnetization damping has to originate from the disorder experienced by the itinerant *s* electrons. As in the case of the itinerant ferromagnets, the susceptibility has to be calculated self-consistently with the magnetization dynamics parametrized by \mathbf{m} . For more details on this model, we refer to Refs. 79 and 68. With the above differences in mind, the following discussion is applicable to both models. The Stoner model is more appropriate for transition-metal ferromagnets because of the strong hybridization between *d* and *s, p* electrons. For dilute magnetic semiconductors with by deep magnetic impurity states the *s-d* model appears to be a better choice.

The single-particle itinerant electron response to electric and magnetic fields in Hamiltonian (53) is all that is needed to compute the magnetization dynamics microscopically. Stoner and *s-d* models have to be distinguished only at the final stages of the calculation, when we self-consistently relate $\mathbf{m}(\mathbf{r}, t)$ to the electron spin response. The final result for the simplest parabolic-band Stoner model with isotropic spin-flip disorder comes down to the torque (11) with $\alpha \approx \beta$. The latter is proportional to the spin-dephasing rate τ_{σ}^{-1} of the itinerant electrons:

$$\beta \approx \frac{\hbar}{\tau_{\sigma} \Delta_{\text{xc}}}. \quad (57)$$

The derivation assumes $\omega, \tau_{\sigma}^{-1} \ll \Delta_{\text{xc}}/\hbar$, which is typically the case in real materials sufficiently below the Curie temperature. The *s-d* model yields the same result for β , Eq. (57), but the Gilbert damping constant

$$\alpha \approx \eta \beta \quad (58)$$

is reduced by the ratio η of the itinerant to the total angular momentum when the *d*-electron spin dynamics is not damped. [Note that Eq. (58) is also valid for the Stoner model since then $\eta = 1$.]

These simple model considerations shed light on the microscopic origins of dissipation in metallic ferromagnet as reflected in the α and β parameters. In Sec. IV we present a more systematic, first-principle approach based on the scattering-matrix approach, which accesses the material dependence of both α and β with realistic electronic band structures.

B. Spin Pumping

1. Discrete Systems

When the scattering matrix is time-dependent, the energy of outgoing and incoming states does not have to be conserved and the scattering relation (40) needs to be appropriately generalized⁸⁰. We will demonstrate here how this is done in the limit of slow magnetization dynamics, *i.e.*, adiabatic pumping. When the time dependence of the scattering matrix $\hat{S}_{\alpha\beta}^{(nm)}[X_i(t)]$ is parameterized by a set of real-valued parameters $X_i(t)$, the pumped spin current in excess of its static bias-driven value (49) is given by¹⁴

$$\mathbf{I}_{\alpha}^s(t) = e \sum_i \frac{\partial \mathbf{n}_{\alpha}}{\partial X_i} \frac{dX_i(t)}{dt}, \quad (59)$$

where the “spin emissivity” vector by the scatterer into lead α is⁸¹

$$\frac{\partial \mathbf{n}_{\alpha}}{\partial X_i} = \frac{1}{2\pi} \text{Im} \sum_{\beta} \sum_{mn} \sum_{ss'\sigma} \frac{\partial S_{\alpha\beta}^{(ms,n\sigma)*}}{\partial X_i} \hat{\sigma}^{(ss')} S_{\alpha\beta}^{(ms',n\sigma)}. \quad (60)$$

Here, $\hat{\sigma}^{(ss')}$ is again the vector of Pauli matrices. In the case of a magnetic monodomain insertion and in the absence of spin-orbit interactions, the spin-dependent scattering matrix between the normal-metal leads can be written in terms of the respective spin-up and spin-down scattering matrices:²¹

$$S_{\alpha\beta}^{(ms,ns')}[\mathbf{m}] = \frac{1}{2} S_{\alpha\beta}^{(mn)\uparrow} \left(\delta^{(ss')} + \mathbf{m} \cdot \hat{\sigma}^{(ss')} \right) + \frac{1}{2} S_{\alpha\beta}^{(mn)\downarrow} \left(\delta^{(ss')} - \mathbf{m} \cdot \hat{\sigma}^{(ss')} \right). \quad (61)$$

Here, $\mathbf{m}(t)$ is the unit vector along the magnetization direction and \uparrow (\downarrow) are spin orientations defined along (opposite) to \mathbf{m} .

Spin pumping due to magnetization dynamics $\mathbf{m}(t)$ is then found by substituting Eq. (61) into Eqs. (60) and (59). After straightforward algebra:¹⁴

$$\mathbf{I}_{\alpha}^s(t) = \left(\frac{\hbar}{e} \right) \left(G_{\perp}^{(R)} \mathbf{m} \times \frac{d\mathbf{m}}{dt} + G_{\perp}^{(I)} \frac{d\mathbf{m}}{dt} \right). \quad (62)$$

As before, we assume here a sufficiently thick ferromagnet, on the scale of the transverse spin-coherence length. Note that the spin pumping is expressed in terms of the same complex-valued mixing conductance $G_{\perp} = G_{\perp}^{(R)} + iG_{\perp}^{(I)}$ as the dc current (49), in agreement with the Onsager reciprocity principle as found on phenomenological grounds in Sec. II C.

Charge pumping is governed by expressions similar to Eqs. (59) and (60), subject to the following substitution: $\hat{\sigma} \rightarrow \delta$ (Kronecker delta). A finite charge pumping by a monodomain magnetization dynamics into normal-metal leads, however, requires a ferromagnetic analyzer or finite spin-orbit interactions and appropriately reduced symmetries, as discussed in Refs. 42,82–84.

An immediate consequence of the pumped spin current (62) is an enhanced Gilbert damping of the magnetization dynamics.¹⁴ Indeed, when the reservoirs are good spin sinks and spin backflow can be disregarded, the spin torque associated with the spin current (62) into the α -th lead, as dictated by the conservation of the spin angular momentum, Eq. (3), contributes (*cf.* Eq. (18)):

$$\alpha' = g^* \frac{\hbar \mu_B}{2e^2} \frac{G_{\perp}^{(R)}}{M_s \mathcal{V}} \quad (63)$$

to the Gilbert damping of the ferromagnet in Eq. (1). Here, $g^* \sim 2$ is the g factor of the ferromagnet, $M_s \mathcal{V}$ its total magnetic moment, and μ_B is Bohr magneton. For simplicity, we neglected $G_{\perp}^{(I)}$, which is usually not important for inter-metallic interfaces. If we disregard energy relaxation processes inside the ferromagnet, which would drain the

associated energy dissipation out of the electronic system, the enhanced energy dissipation associated with the Gilbert damping is associated with heat flows into the reservoirs. Phenomenologically, the dissipation power follows from the magnetic free energy F and the LLG Eq. (1) as

$$P \equiv -\partial_{\mathbf{m}} F_m \cdot \dot{\mathbf{m}} = M_s \mathcal{V} \mathbf{H}_{\text{eff}} \cdot \dot{\mathbf{m}} = \frac{\alpha M_s \mathcal{V}}{\gamma} \dot{\mathbf{m}}^2 \quad (64)$$

or, more generally, for anisotropic damping (with, for simplicity, an isotropic gyromagnetic ratio), by

$$P = \frac{M_s \mathcal{V}}{\gamma} \dot{\mathbf{m}} \cdot \overleftrightarrow{\alpha} \cdot \dot{\mathbf{m}}. \quad (65)$$

Heat flows can be also calculated microscopically by the scattering-matrix transport formalism. At low temperatures, the heat pumping rate into the α -th lead is given by^{85–87}

$$I_\alpha^E = \frac{\hbar}{4\pi} \sum_\beta \sum_{mn} \sum_{ss'} \left| \hat{S}_{\alpha\beta}^{(ms,ns')} \right|^2 = \frac{\hbar}{4\pi} \sum_\beta \text{Tr} \left(\hat{S}_{\alpha\beta}^\dagger \hat{S}_{\alpha\beta} \right), \quad (66)$$

where the carets denote scattering matrices with suppressed transverse-channel indices. When the time dependence is entirely due to the magnetization dynamics, $\hat{S}_{\alpha\beta}^{(ms,ns')} = \partial_{\mathbf{m}} S_{\alpha\beta}^{(ms,ns')} \cdot \dot{\mathbf{m}}$. Utilizing again Eq. (61), we find for the heat current into the α -th lead:⁸⁸

$$I_\alpha^E = \dot{\mathbf{m}} \cdot \overleftrightarrow{G}_\alpha \cdot \dot{\mathbf{m}}, \quad (67)$$

in terms of the dissipation tensor⁸⁸

$$G_\alpha^{ij} = \frac{\gamma^2 \hbar}{4\pi} \text{Re} \sum_\beta \text{Tr} \left(\frac{\partial \hat{S}_{\alpha\beta}^\dagger}{\partial m_i} \frac{\partial \hat{S}_{\alpha\beta}}{\partial m_j} \right) \quad (68)$$

In the limit of vanishing spin-flip in the ferromagnet, meaning that all dissipation takes place in the reservoirs, we find

$$G_\alpha^{ij} = \frac{\gamma^2 \hbar}{4\pi} \text{Re} \sum_\beta \text{Tr} \left(\frac{\partial \hat{S}_{\alpha\beta}^\dagger}{\partial m_i} \frac{\partial \hat{S}_{\alpha\beta}}{\partial m_j} \right) = \gamma^2 \frac{1}{2} \left(\frac{\hbar}{e} \right)^2 G_\perp^{(R)} \delta_{ij}. \quad (69)$$

Equating this I_α^E with P above, we obtain a microscopic expression for the Gilbert damping tensor $\overleftrightarrow{\alpha}$:

$$\overleftrightarrow{\alpha} = g^* \frac{\hbar \mu_B}{2e^2} \frac{G_\perp^{(R)}}{M_s \mathcal{V}} \overleftrightarrow{1}, \quad (70)$$

which agrees with Eq. (63). Indeed, in the absence of spin-orbit coupling the damping is necessarily isotropic. While Eq. (63) reproduces the additional Gilbert damping due to the interfacial spin pumping, Eq. (69) is more general, and can be used to compute bulk magnetization damping, as long as it is of a purely electronic origin^{88,89}.

2. Continuous Systems

As has already been noted, spin pumping in continuous systems is the Onsager counterpart of the spin-transfer torque discussed in Sec. III A 2.³¹ While a direct diagrammatic calculation for this pumping is possible⁵⁴, with results equivalent to those of the quantum-kinetic description of the spin-transfer torque outlined above, we believe that the scattering-matrix formalism is the most powerful microscopic approach³². The latter is particularly suitable for implementing parameter-free computational schemes that allow a realistic description of material-dependent properties.

An important example is pumping by a moving domain wall in a quasi-one-dimensional ferromagnetic wire. When the domain wall is driven by a weak magnetic field, its shape remains to a good approximation unaffected, and only its position $r_w(t)$ along the wire is needed to parameterize its slow dynamics. The electric current pumped by the sliding domain wall into the α -th lead can then be viewed as pumping by the r_w parameter, which leads to⁸¹

$$I_\alpha^c = \frac{e \dot{r}_w}{2\pi} \text{Im} \sum_\beta \text{Tr} \left(\frac{\partial \hat{S}_{\alpha\beta}}{\partial r_w} \hat{S}_{\alpha\beta}^\dagger \right). \quad (71)$$

The total heat flow into both leads induced by this dynamics is according to Eq. (66)

$$I^E = \frac{\hbar \dot{r}_w^2}{4\pi} \sum_{\alpha\beta} \text{Tr} \left(\frac{\partial \hat{S}_{\alpha\beta}^\dagger}{\partial r_w} \frac{\partial \hat{S}_{\alpha\beta}}{\partial r_w} \right). \quad (72)$$

Evaluating the scattering-matrix expressions on the right-hand side of the above equations leads to microscopic magnetotransport response coefficients that describe the interaction of the domain wall with electric currents, including spin transfer and pumping effects.

These results leads to microscopic expressions for the phenomenological response³² of the domain-wall velocity \dot{r}_w and charge current I^c to a voltage V and magnetic field applied along the wire H :

$$\begin{pmatrix} \dot{r}_w \\ I^c \end{pmatrix} = \begin{pmatrix} L_{ww} & L_{wc} \\ L_{cw} & L_{cc} \end{pmatrix} \begin{pmatrix} 2AM_s H \\ V \end{pmatrix}, \quad (73)$$

subject to appropriate conventions for the signs of voltage and magnetic field and assuming a head-to-head or tail-to-tail wall such that the magnetization outside of the wall region is collinear with the wire axis. $2AM_s H$ is the thermodynamic force normalized to the entropy production by the magnetic system, where A is the cross-sectional area of the wire. We may therefore expect the Onsager's symmetry relation $L_{cw} = L_{wc}$. When a magnetic field moves the domain wall in the absence of a voltage $I^c = (L_{cw}/L_{ww})\dot{r}_w$, which, according to Eq. (71) leads to the ratio L_{cw}/L_{ww} in terms of the scattering matrices. The total energy dissipation for the same process is $I^E = \dot{r}_w^2/L_{ww}$, which, according to Eq. (72), establishes a scattering-matrix expression for L_{ww} alone. By supplementing these equations with the standard Landauer-Büttiker formula for the conductance

$$G = \frac{e^2}{h} \text{Tr} \left(\hat{S}_{12}^\dagger \hat{S}_{12} \right), \quad (74)$$

valid in the absence of domain-wall dynamics, we find L_{cc} in the same spirit since $G = L_{cc} - L_{wc}^2/L_{ww}$. Summarizing, the phenomenological response coefficients in Eq. (73) read³²:

$$L_{ww}^{-1} = \frac{\hbar}{4\pi} \sum_{\alpha\beta} \text{Tr} \left(\frac{\partial \hat{S}_{\alpha\beta}^\dagger}{\partial r_w} \frac{\partial \hat{S}_{\alpha\beta}}{\partial r_w} \right), \quad (75)$$

$$L_{cw} = L_{wc} = L_{ww} \frac{e}{2\pi} \text{Im} \sum_{\beta} \text{Tr} \left(\frac{\partial \hat{S}_{\alpha\beta}}{\partial r_w} \hat{S}_{\alpha\beta}^\dagger \right), \quad (76)$$

$$L_{cc} = \frac{e^2}{h} \text{Tr} \left(\hat{S}_{12} \hat{S}_{12}^\dagger \right) + \frac{L_{wc}^2}{L_{ww}}. \quad (77)$$

When the wall is sufficiently smooth, we can model spin torques and pumping by the continuum theory based on the gradient expansion in the magnetic texture, Eqs. (11) and (12). Solving for the magnetic-field and current-driven dynamics of such domain walls is then possible using the Walker ansatz^{72,90}. Introducing the domain-wall width λ_w :

$$\alpha = \frac{\gamma \lambda_w}{2AM_s L_{ww}} \quad \text{and} \quad \beta = -\frac{e \lambda_w}{\hbar P G} \frac{L_{wc}}{L_{ww}}. \quad (78)$$

When the wall is sharp the adiabatic approximation underlying the leading-order gradient expansion breaks down. These relations can still be used as definitions of the effective domain-wall α and β . As such, these could be distinct from the bulk values that are associated with smooth textures. This is relevant for dilute magnetic semiconductors, for which the adiabatic approximation easily breaks down³². In transition-metal ferromagnets, on the other hand, the adiabatic approximation is generally perceived to be a good starting point, and we may expect the dissipative parameters in Eq. (78) to be comparable to their bulk values discussed in Sec. III A 2.

IV. FIRST-PRINCIPLES CALCULATIONS

We have shown that the essence of spin pumping and spin transfer can be captured by a small number of phenomenological parameters. In this section we address the material dependence of these phenomena in terms of the (reflection) mixing conductance G_{\perp} , the dimensionless Gilbert damping parameter α , and the out-of-plane torque parameter β .

For discrete systems the (reflection) mixing conductance G_{\perp} was studied theoretically by Xia *et al.*⁹¹, Zwierzycki *et al.*⁴⁵ and Carva *et al.*⁹². G_{\perp} describes the spin current flowing in response to an externally applied spin accumulation $e\mathbf{V}_s$ that is a vector with length equal to half of the spin-splitting of the chemical potentials $e|\mathbf{V}_s| = e(V_{\uparrow} - V_{\downarrow})/2$. It also describes the spin torque exerted on the moment of the magnetic layer^{9,21,45,91-94}. Consider a spin accumulation in a normal metal N , which is in contact with a ferromagnet on the right magnetized along the z axis. The spin current incident on the interface is proportional to the number of incident channels in the left lead, $\mathbf{I}_{\text{in}}^N = 2G_{\text{N}}^{\text{Sh}}\mathbf{V}_s$, while the reflected spin current is given by

$$\mathbf{I}_{\text{out}}^N = 2 \begin{pmatrix} G_{\text{N}}^{\text{Sh}} - G_{\perp}^{(R)} & -G_{\perp}^{(I)} & 0 \\ G_{\perp}^{(I)} & G_{\text{N}}^{\text{Sh}} - G_{\perp}^{(R)} & 0 \\ 0 & 0 & G_{\text{N}}^{\text{Sh}} - \frac{G_{\uparrow} + G_{\downarrow}}{2} \end{pmatrix} \mathbf{V}_s, \quad (79)$$

where G_{σ} are the conventional Landauer-Büttiker conductances. The real and imaginary parts of $G_{\text{N}}^{\text{Sh}} - G_{\perp} = (e^2/h) \sum_{mn} r_{mn}^{\uparrow} r_{mn}^{\downarrow*}$ are related to the components of the reflected transverse spin current and can be calculated by considering a single N|F interface⁹¹. When the ferromagnet is a layer with finite thickness d sandwiched between normal metals, the reflection mixing conductance depends on d and it is necessary to consider also the transmission mixing conductance $(e^2/h) \sum_{mn} t_{mn}^{\uparrow} t_{mn}^{\downarrow*}$. In Ref. 45, both reflection and transmission mixing conductances were calculated for Cu|Co|Cu and Au|Fe|Au sandwiches as a function of magnetic layer thickness d . The real and imaginary parts of the transmission mixing conductance and the imaginary part of the reflection mixing conductance were shown to decay rapidly with increasing d implying that the absorption of the transverse component of the spin current occurs within a few monolayers of the N|F interface for ideal lattice matched interfaces. When a minimal amount of interface disorder was introduced the absorption increased. The limit $G_{\perp} \rightarrow G_{\text{N}}^{\text{Sh}}$ corresponds to the situation where all of the incoming transverse polarized spin current is absorbed in the magnetic layer. The torque is then proportional to the Sharvin conductance of the normal metal. This turns out to be the situation for all but the thinnest (few monolayers) and cleanest Co and Fe magnetic layers considered by Zwierzycki *et al.*⁴⁵ However, when there is nesting between Fermi surface sheets for majority and minority spins so that both spins have the same velocities over a large region of reciprocal space, then the transverse component of the spin current does not damp so rapidly and G_{\perp} can continue to oscillate for large values of d . This has been found to occur for ferromagnetic Ni in the (001) direction.⁹²

Eq. 17 implies that the spin pumping renormalizes both the Gilbert damping parameter α and the gyromagnetic ratio γ of a ferromagnetic film embedded in a conducting non-magnetic medium. However, in view of the results discussed in the previous paragraph, we conclude that the main effect of the spin pumping is to enhance the Gilbert damping. The correction is directly proportional to the real part of the reflection mixing conductance and is essentially an interface property. Oscillatory effects are averaged out for realistic band structures, especially in the presence of disorder. $G_{\perp}^{(R)}$ determines the damping enhancement of a single ferromagnetic film embedded in a perfect spin-sink medium and is usually very close to G_{N}^{Sh} for intermetallic interfaces^{91,93}.

A. Alpha

We begin with a discussion of the small-angle damping measured as a function of temperature using ferromagnetic resonance (FMR). There is general agreement that spin-orbit coupling and disorder are essential ingredients in any description of how spin excitations relax to the ground state. In the absence of intrinsic disorder, one might expect the damping to increase monotonically with temperature in clean magnetic materials and indeed, this is what is observed for Fe. Heinrich *et al.*⁹⁵ developed an explicit model for this high-temperature behaviour in which itinerant s electrons scatter from localized d moments and transfer spin angular momentum to the lattice via spin-orbit interaction. This $s-d$ model results in a damping that is inversely proportional to the electronic relaxation time, $\alpha \sim 1/\tau$, i.e., is *resistivity*-like. However, at low temperatures, both Co and Ni exhibit a sharp rise in damping as the temperature decreases. The so-called breathing Fermi surface model was proposed⁹⁶⁻⁹⁸ to describe this low-temperature *conductivity*-like damping, $\alpha \sim \tau$. In this model the electronic population lags behind the instantaneous equilibrium distribution due to the precessing magnetization and requires dissipation of energy and angular momentum to bring the system back to equilibrium.

Of the numerous microscopic models that have been proposed⁹⁹ to explain the damping behaviour of metals, only the so-called ‘torque correlation model’ (TCM)¹⁰⁰ is qualitatively successful in explaining the non-monotonic damping observed for hcp Co that results from conductivity-like and resistivity-like behaviours at low and high temperatures, respectively. The central result of the TCM is the expression

$$\tilde{G} = \frac{g^2 \mu_B^2}{\hbar} \sum_{n,m} \int \frac{d\mathbf{k}}{(2\pi)^3} \left| \langle n, \mathbf{k} | [\sigma_-, \hat{\mathcal{H}}_{so}] | m, \mathbf{k} \rangle \right|^2 W_{n,m}(\mathbf{k}) \quad (80)$$

for the damping. The commutator $[\sigma_-, \hat{\mathcal{H}}_{so}]$ describes a torque between the spin and orbital moments that arises as the spins precess. The corresponding matrix elements in (80) describe transitions between states in bands n and m induced by this torque whereby the crystal momentum \mathbf{k} is conserved. Disorder enters in the form of a phenomenological relaxation time τ via the spectral overlap

$$W_{n,m}(\mathbf{k}) = -\frac{1}{\pi} \int A_n(\varepsilon, \mathbf{k}) A_m(\varepsilon, \mathbf{k}) \frac{df}{d\varepsilon} d\varepsilon \quad (81)$$

where the electron spectral function $A_n(\varepsilon, \mathbf{k})$ is a Lorentzian centred on the band n , whose width is determined by the scattering rate. For intraband transitions with $m = n$, integration over energy yields a spectral overlap which is proportional to the relaxation time, like the conductivity. For interband transitions with $m \neq n$, the energy integration leads to a spectral overlap that is roughly inversely proportional to the relaxation time, like the resistivity.

To interpret results obtained with the TCM, Gilmore et al.^{100–104} used an effective field approach expressing the effective field about which the magnetization precesses in terms of the total energy

$$\mu_0 \mathbf{H}^{\text{eff}} = -\frac{\partial E}{\partial \mathbf{M}} \quad (82)$$

and then approximated the total energy by a sum of single particle eigenvalues $E \sim \sum_{n,\mathbf{k}} \varepsilon_{n\mathbf{k}} f_{n\mathbf{k}}$, so that the effective field naturally splits into two parts

$$\mathbf{H}^{\text{eff}} = \frac{1}{\mu_0 M} \sum_{n,\mathbf{k}} \left[\frac{\partial \varepsilon_{n\mathbf{k}}}{\partial \mathbf{m}} f_{n\mathbf{k}} + \varepsilon_{n\mathbf{k}} \frac{\partial f_{n\mathbf{k}}}{\partial \mathbf{m}} \right] \quad (83)$$

the first of which corresponds to the breathing Fermi surface model, intraband transitions and conductivity-like behaviour while the second term could be related to interband transitions and resistivity-like behaviour. Evaluation of this model for Fe, Co and Ni using first-principles calculations to determine $\varepsilon_{n\mathbf{k}}$ including spin-orbit coupling yields results for the damping α in good qualitative and reasonable quantitative agreement with the experimental observations.¹⁰¹

In spite of this real progress, the TCM has disadvantages. As currently formulated, the model can only be applied to periodic lattices. Extending it to handle inhomogeneous systems such as ferromagnetic substitutional alloys like Permalloy ($\text{Ni}_{80}\text{Fe}_{20}$), magnetic multilayers or heterojunctions, disordered materials or materials with surfaces is far from trivial. The TCM incorporates disorder in terms of a relaxation time parameter τ and so suffers from the same disadvantages as all transport theories similarly formulated, namely, that it is difficult to relate microscopically measured disorder unambiguously to a given value of τ . Indeed, since τ in general depends on incoming and scattered band index n , wave vector \mathbf{k} , as well as spin index, assuming a single value for it is a gross simplification. A useful theoretical framework should allow us to study not only crystalline materials such as the ferromagnetic metals Fe, Co and Ni and substitutional disordered alloys such as permalloy (Py), but also amorphous materials and configurations such as magnetic heterojunctions, multilayers, thin films etc. which become more important and are more commonly encountered as devices are made smaller.

The scattering theoretical framework discussed in section IIIB satisfies these requirements and has recently been implemented by extending a first-principles scattering formalism^{105,106} based upon the local spin density approximation (LSDA) of density functional theory (DFT) to include non-collinearity, spin-orbit coupling (SOC) and chemical or thermal disorder on equal footings.⁸⁹ Relativistic effects are included by using the Pauli Hamiltonian. To calculate the scattering matrix, a “wave-function matching” (WFM) scheme^{105–107} implemented with a minimal basis of tight-binding linearized muffin-tin orbitals (TB-LMTOs)^{108,109}. Atomic-sphere-approximation (ASA) potentials^{108,109} are calculated self-consistently using a surface Green’s function (SGF) method also implemented¹¹⁰ with TB-LMTOs.

1. NiFe alloys.

The flexibility of the scattering theoretical formulation of transport can be demonstrated with an application to NiFe binary alloys.⁸⁹ Charge and spin densities for binary alloy A and B sites are calculated using the coherent potential approximation (CPA)¹¹¹ generalized to layer structures¹¹⁰. For the transmission matrix calculation, the resulting spherical potentials are distributed at random in large lateral supercells (SC) subject to maintenance of the appropriate concentration of the alloy^{105,106}. Solving the transport problem using lateral supercells makes it possible to go beyond effective medium approximations such as the CPA. As long as one is only interested in the properties of bulk alloys, the leads can be chosen for convenience and Cu leads with a single scattering state for each value of crystal momentum, \mathbf{k}_{\parallel} are very convenient. The alloy lattice constants are determined using Vegard’s law and the

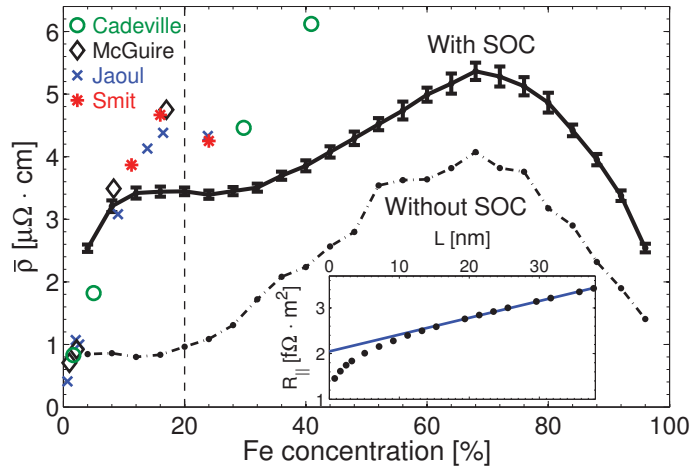


FIG. 4: Calculated resistivity as a function of the concentration x for fcc $\text{Ni}_{1-x}\text{Fe}_x$ binary alloys with (solid line) and without (dashed-dotted line) SOC. Low temperature experimental results are shown as symbols^{114–117}. The composition $\text{Ni}_{80}\text{Fe}_{20}$ is indicated by a vertical dashed line. Inset: resistance of $\text{Cu}|\text{Ni}_{80}\text{Fe}_{20}|\text{Cu}$ as a function of the thickness of the alloy layer. Dots indicate the calculated values averaged over five configurations while the solid line is a linear fit.

lattice constants of the leads are made to match. Though NiFe is fcc only for the concentration range $0 \leq x \leq 0.6$, the fcc structure is used for all values of x .

To illustrate the methodology, we begin by calculating the electrical resistivity of $\text{Ni}_{80}\text{Fe}_{20}$. In the Landauer-Büttiker formalism, the conductance can be expressed in terms of the transmission matrix t as $G = (e^2/h)\text{Tr}\{tt^\dagger\}$ ^{112,113}. The resistance of the complete system consisting of ideal leads sandwiching a layer of ferromagnetic alloy of thickness L is $R(L) = 1/G(L) = 1/G_{\text{Sh}} + 2R_{\text{if}} + R_{\text{b}}(L)$ where $G_{\text{Sh}} = (2e^2/h)N$ is the Sharvin conductance of each lead with N conductance channels per spin, R_{if} is the interface resistance of a single N|F interface, and $R_{\text{b}}(L)$ is the bulk resistance of a ferromagnetic layer of thickness L ^{66,106}. When the ferromagnetic slab is sufficiently thick, Ohmic behaviour is recovered whereby $R_{\text{b}}(L) \approx \rho L$ as shown in the inset to Fig. 4 and the bulk resistivity ρ can be extracted from the slope of $R(L)$. For currents parallel and perpendicular to the magnetization direction, the resistivities are different and have to be calculated separately. The average resistivity is given by $\bar{\rho} = (\rho_{\parallel} + 2\rho_{\perp})/3$, and the anisotropic magnetoresistance ratio (AMR) by $(\rho_{\parallel} - \rho_{\perp})/\bar{\rho}$.

For $\text{Ni}_{80}\text{Fe}_{20}$ we find values of $\bar{\rho} = 3.5 \pm 0.15 \mu\text{Ohm-cm}$ and $\text{AMR} = 19 \pm 1\%$, compared to experimental low-temperature values in the range $4.2 - 4.8 \mu\text{Ohm-cm}$ for $\bar{\rho}$ and 18% for AMR¹¹⁴. The resistivity calculated as a function of x is compared to low temperature literature values^{114–117} in Fig. 4. The overall agreement with previous calculations is good^{118,119}. In spite of the smallness of the SOC, the resistivity of Py is underestimated by more than a factor of four when it is omitted, underlining its importance for understanding transport properties.

Assuming that the Gilbert damping is isotropic for cubic substitutional alloys and allowing for the enhancement of the damping due to the F|N interfaces^{14,17,18,45,120,121}, the total damping in the system with a ferromagnetic slab of thickness L can be written $\tilde{G}(L) = \tilde{G}_{\text{if}} + \tilde{G}_{\text{b}}(L)$ where we express the bulk damping in terms of the dimensionless Gilbert damping parameter $\tilde{G}_{\text{b}}(L) = \alpha\gamma M_s(L) = \alpha\gamma\mu_s AL$, where μ_s is the magnetization density and A is the cross section. The results of calculations for $\text{Ni}_{80}\text{Fe}_{20}$ are shown in the inset to Fig. 5. The intercept at $L = 0$, \tilde{G}_{if} , allows us to extract the damping enhancement⁴⁵ but here we focus on the bulk properties and leave consideration of the material dependence of the interface enhancement for later study. The value of α determined from the slope of $\tilde{G}(L)/(\gamma\mu_s A)$ is 0.0046 ± 0.0001 that is at the lower end of the range of values $0.004 - 0.013$ measured at room temperature for Py^{17,18,120–131}.

Fig. 5 shows the Gilbert damping parameter as a function of x for $\text{Ni}_{1-x}\text{Fe}_x$ binary alloys in the fcc structure. From a large value for clean Ni, it decreases rapidly to a minimum at $x \sim 0.65$ and then grows again as the limit of clean fcc Fe is approached. Part of the decrease in α with increasing x can be explained by the increase in the magnetic moment per atom as we progress from Ni to Fe. The large values of α calculated in the dilute alloy limits can be understood in terms of conductivity-like enhancement at low temperatures^{132,133} that has been explained in terms of intraband scattering^{100–102,104}. The trend exhibited by the theoretical $\alpha(x)$ is seen to be reflected by experimental results obtained at room temperature. In spite of a large spread in measured values, these seem to be systematically larger than the calculated values. Part of this discrepancy can be attributed to an increase in α with temperature^{122,134}.

Calculating α for the end members, Ni and Fe, of the substitutional alloy $\text{Ni}_{1-x}\text{Fe}_x$ presents a practical problem. In

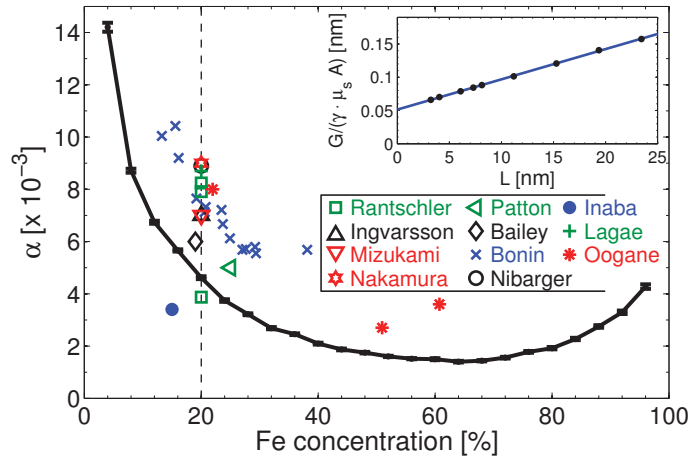


FIG. 5: Calculated zero temperature (solid line) and experimental room temperature (symbols) values of the Gilbert damping parameter as a function of the concentration x for fcc $\text{Ni}_{1-x}\text{Fe}_x$ binary alloys^{17,18,120–131}. Inset: total damping of $\text{Cu}[\text{Ni}_{80}\text{Fe}_{20}]\text{Cu}$ as a function of the thickness of the alloy layer. Dots indicate the calculated values averaged over five configurations while the solid line is a linear fit.

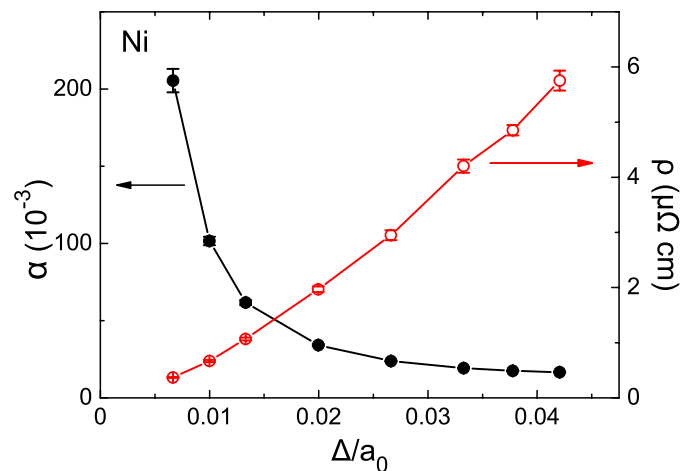


FIG. 6: Calculated Gilbert damping and resistivity for fcc Ni as function of the relative RMS displacement with respect to the corresponding lattice constant, $a_0 = 3.524 \text{ \AA}$.

these limits there is no scattering whereas in experiment there will always be some residual disorder at low temperatures and at finite temperatures, electrons will scatter from the thermally displaced ions. We introduce a simple “frozen thermal disorder” scheme to study Ni and Fe and simulate the effect of temperature via electron-phonon coupling by using a random Gaussian distribution of ionic displacements \mathbf{u}_i , corresponding to a harmonic approximation. This is characterized by the root-mean-square (RMS) displacement $\Delta = \sqrt{\langle |\mathbf{u}_i|^2 \rangle}$ where the index i runs over all atoms. Typical values will be of the order of a few hundredths of an angstrom. We will not attempt to relate Δ to a real lattice temperature here.

We calculate the total resistance $R(L)$ and Gilbert damping $\tilde{G}(L)$ for thermally disordered scattering regions of variable length L and extract the resistivity ρ and damping α from the slopes as before. The results for Ni are shown as a function of the RMS displacement in Fig. 6. The resistivity is seen to increase monotonically with Δ underlining the correlation between Δ and a real temperature. For large values of Δ , α saturates for Ni in agreement with experiment¹³² and calculations based on the torque-correlation model^{101,103,104} where no concrete scattering mechanism is attached to the relaxation time τ . The absolute value of the saturated α is about 70% of the observed value. For small values of Δ , the Gilbert damping increases rapidly as Δ decreases. This sharp rise corresponds to the experimentally observed conductivity-like behaviour at low temperatures and confirms that the scattering formalism can reproduce this feature.

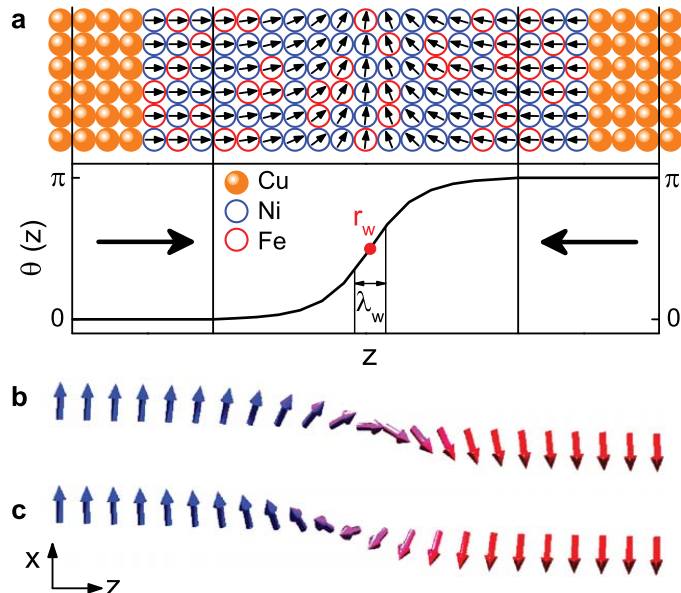


FIG. 7: (a) Sketch of the configuration of a Néel DW in Py sandwiched by two Cu leads. The arrows denotes local magnetization directions. The curve shows the mutual angle between the local magnetization and the transport direction (z axis). (b) Magnetization profile of the rotated Néel wall. (c) Magnetization profile of the Bloch wall.

B. Beta

To evaluate expressions (78) for the out-of-plane spin-torque parameter β given in Section IIIB requires modelling domain walls (DW) in the scattering region sandwiched between ideal Cu leads. A head-to-head Néel DW is introduced inside the permalloy region by rotating the local magnetization to follow the Walker profile, $\mathbf{m}(z) = [f(z), 0, g(z)]$ with $f(z) = \cosh^{-1}[(z - r_w)/\lambda_w]$ and $g(z) = -\tanh[(z - r_w)/\lambda_w]$ as shown schematically in Fig. 7(a). r_w is the DW center and λ_w is a parameter characterizing its width. In addition to the Néel wall, we also study a rotated Néel wall with magnetization profile $\mathbf{m}(z) = [g(z), 0, f(z)]$ sketched in Fig. 7(b) and a Bloch wall with $\mathbf{m}(z) = [g(z), f(z), 0]$ sketched in Fig. 7(c).

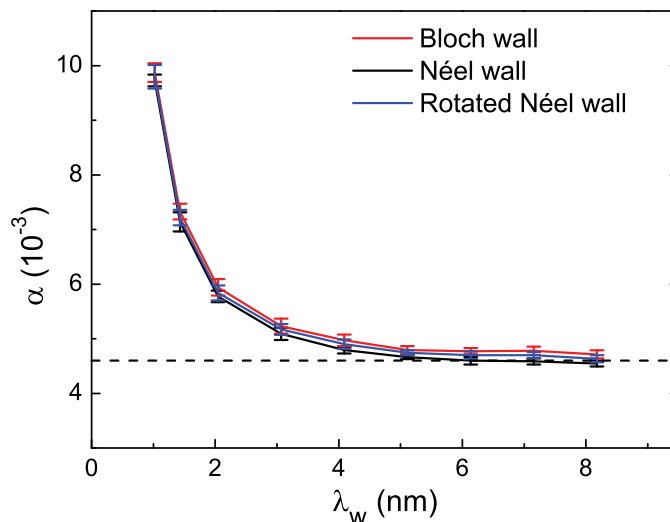


FIG. 8: Calculated effective Gilbert damping constant α for Py DWs as a function of λ_w . The dashed lines show the calculated α for bulk Py with the magnetization parallel to the transport direction⁸⁹.

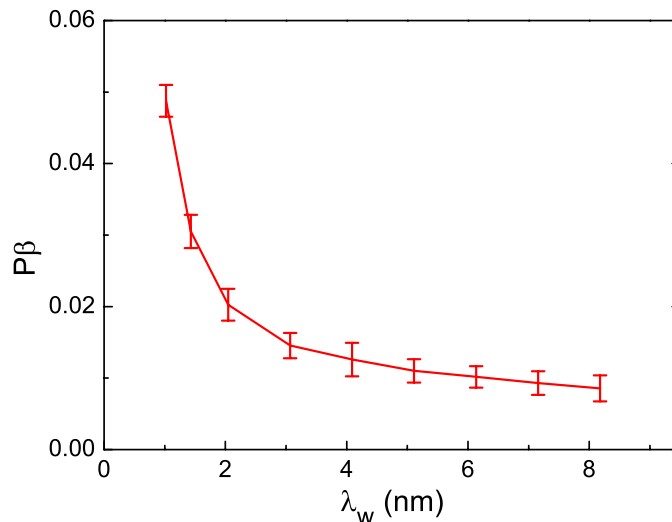


FIG. 9: Calculated out-of-plane spin torque parameter $P\beta$ for permalloy DWs as a function of λ_w .

The effective Gilbert damping constant α of permalloy in the presence of all three DWs calculated using (78) is shown in Fig. 8. For different types of DWs, α is identical within the numerical accuracy indicating that the Gilbert damping is isotropic due to the strong impurity scattering¹⁰³. In the adiabatic limit, α saturates to the same value (the dashed lines in Fig. 8) calculated for bulk permalloy using (68). It implies that the DWs in permalloy have little effect on the magnetization relaxation and the strong impurity scattering is the dominant mechanism to release energy and magnetization. This is in contrast to DWs in (Ga,Mn)As where Gilbert damping is mostly contributed by the reflection of the carriers from the DW.³² At $\lambda_w < 5$ nm, the non-adiabatic reflection of conduction electrons due to the rapidly-varying magnetization direction becomes significant and results in a sharp rise in α for narrow DWs.

The out-of-plane torque is formulated as $\beta(\hbar\gamma P/2eM_s)\mathbf{m} \times (\mathbf{j} \cdot \nabla)\mathbf{m}$ in the Landau-Lifshitz-Gilbert (LLG) equation under a finite current density \mathbf{j} . In principle, the current polarization P is required to determine β . Since the spin-dependent conductivities of permalloy depend on the angle between the current and the magnetization, P is not well-defined for magnetic textures. Instead, we calculate the quantity $P\beta$, as shown in Fig. 9 for a Bloch DW. For $\lambda_w < 5$ nm, $P\beta$ decreases quite strongly with increasing λ_w corresponding to an expected non-adiabatic contribution to the out-of-plane torque. This arises from the spin-flip scattering induced by the rapidly-varying magnetization in narrow DWs¹³⁵ and does not depend on the specific type of DW. For $\lambda_w > 5$ nm, which one expects to be in the adiabatic limit, $P\beta$ decreases slowly to a constant value^{27,32,53,69,78,135–143}. It is unclear what length scale is varying so slowly. Unfortunately, the spread of values for different configurations is quite large for the last data point and our best estimate of $P\beta$ for a Bloch DW in permalloy is ~ 0.08 . Taking the theoretical value of $P \sim 0.7$ for permalloy⁸⁹, our best estimate of β is a value of ~ 0.01 .

V. THEORY VERSUS EXPERIMENTS

Spin-torque induced magnetization dynamics in multilayers and its reciprocal effect, the spin pumping, are experimentally well established and quantitatively understood within the framework described in this paper, and need not to be discussed further here.^{15,20} Recent FMR experiments also confirm the spin-pumping contribution to the enhanced magnetization dissipation¹⁴⁴. Spin-pumping occurs in magnetic insulators as well^{7,145}.

The parameters that control the current-induced dynamics of continuous textures are much less well known. Most experiments are carried out on permalloy (Py). It is a magnetically very soft material with large domain wall widths of the order of 100 nm. Although the adiabatic approximations appears to be a safe assumption in Py, many systems involve vortex domain walls with large gradients in the wall center, and, therefore, possibly sizable nonadiabatic corrections. Effective description for such vortex dynamics has been constructed in Ref. 62, where it was shown, in particular, that self-consistent quadratic corrections to damping (which stem from self-pumped currents inducing backaction on the magnetic order) is generally non-negligible in transition-metal ferromagnets.

Early experimental studies^{146,147} for the torque-supplemented [Eq. (11)] LLG equation describing current-driven domain-wall motion in magnetic wires reported values of the β/α ratios in Py close to unity, in agreement with simple

Stoner-model calculations. However, much larger values $\beta/\alpha \sim 8$ was extracted from the current-induced oscillatory motion of domain walls.¹⁴⁸ The inequality $\beta \neq \alpha$ was also inferred from a characteristic transverse to vortex wall structure transformation, although no exact value of the ratio was established.¹⁴⁹ In Ref.¹⁵⁰, vanadium doping of Py was shown to enhance β up to nearly 10α , with little effect on α itself. Even larger ratios, $\beta/\alpha \sim 20$, were found for magnetic vortex motion by an analysis of their displacement as a function of an applied dc current in disc structures.^{151,152}

Eltschka *et al.*¹⁵³ reported on a measurement of the dissipative spin-torque parameter β entering Eq. (11), as manifested by a thermally-activated motion of transverse and vortex domain walls in Py. They found the ratio $\beta_v/\beta_t \sim 7$ for the vortex vs transverse wall, attributing the larger β to high magnetization gradients in the vortex wall core. Their ratio $\beta_t/\alpha \sim 1.3$ turns out to be close to unity, where α is the bulk Gilbert damping. The importance of large spin-texture gradients on the domain-wall and vortex dynamics was theoretically discussed in Refs. 60,62.

The material dependence of the current-induced torques is not yet well investigated. A recent study on CoNi and FePt wires with perpendicular magnetization found $\beta \approx \alpha$, in spite of the relatively narrow domain walls in these materials.¹⁵⁴ Current-induced domain-wall dynamics in dilute magnetic semiconductors¹⁵⁵ generally exhibit similar phenomenology, but a detailed discussion, especially of the domain wall creep regime that can be accessed in these systems, is beyond the scope of this review.

Finally, the first term in the spin-pumping expression (12) has been measured by Yang *et al.*¹⁵⁶ for a domain wall moved by an applied magnetic field above the Walker breakdown field. These experiments confirmed the existence of pumping effects in magnetic textures, which are Onsager reciprocal of spin torques and thus expected on general grounds. Similar experiments carried out below the Walker breakdown would also give direct access to the β parameter.

VI. CONCLUSIONS

A spin polarized current can excite magnetization dynamics in ferromagnets via spin-transfer torques. The reciprocal phenomena is spin-pumping where a dynamic magnetization pumps spins into adjacent conductors. We have discussed how spin-transfer torques and spin-pumping are directly related by Onsager reciprocity relations.

In layered normal metal-ferromagnet systems, spin-transfer torques can be expressed in terms of two conductance parameters governing the flow of spins transverse to the magnetization direction and the spin-accumulation in the normal metal. In metallic systems, the field-like torque is typically much smaller than the effective energy gain/damping torque, but in tunnel systems they might become comparable. Spin-pumping is controlled by the same transverse conductance parameters as spin-transfer torques, the magnetization direction and its rate of change. It can lead to an enhanced magnetization dissipation in ultra-thin ferromagnets or a build-up of spins, a spin-battery, in normal metals where the spin-flip relaxation rate is low.

Spin-transfer torque and spin-pumping phenomena in magnetization textures are similar to their counterparts in layered normal metal-ferromagnet systems. A current becomes spin polarized in a ferromagnet and this spin-polarized current in a magnetization texture gives rise to a reactive torque and a dissipative torque in the lowest gradient expansion. The reciprocal pumping phenomena can be viewed as an electromotive force, the dynamic magnetization texture pumps a spin-current that in turn is converted to a charge current or voltage by the giant magnetoresistance effect. Naturally, the parameters governing the spin-transfer torques and the pumping phenomena are also the same in continuously textured ferromagnets.

When the spin-orbit interaction becomes sufficiently strong, additional effects arise in the coupling between the magnetization and itinerant electrical currents. A charge potential can then by itself induce a torque on the ferromagnet and the reciprocal phenomena is that a precessing ferromagnet can induce a charge current in the adjacent media. The latter can be an alternative way to carry out FMR measurements on small ferromagnets by measuring the induced voltage across a normal metal-ferromagnet-normal metal device.

These phenomena are well-know and we have reviewed them in a unified physical picture and discussed the connection between these and some experimental results.

Acknowledgments

We are grateful to Jørn Foros, Bertrand I. Halperin, Kjetil M. D. Hals, Alexey Kovalev, Yi Liu, Hans Joakim Skadsem, Anton Starikov, Zhe Yuan, and Maciej Zwierzycki for discussions and collaborations.

This work was supported in part by EU-ICT-7 contract no. 257159 MACALO - Magneto Caloritronics, DARPA,

and NSF under Grant No. DMR-0840965.

-
- ¹ S.D. Bader and S.S.P. Parkin, *Spintronics*, Annual Review of Condensed Matter Physics **1**, 71 (2010).
 - ² T. J. Silva and W. H. Rippard, *Developments in nano-oscillators based upon spin-transfer point-contact devices*, J. Magn. Magn. Mater. **320**, 1260 (2008).
 - ³ P M Braganca , B A Gurney , B A Wilson , J A Katine , S Maat and J R Childress, *Nanoscale magnetic field detection using a spin torque oscillator*, Nanotechnology **21** 235202 (2010)
 - ⁴ S. Matsunaga, K. Hiyama, A. Matsumoto, S. Ikeda, H. Hasegawa, K. Miura, J. Hayakawa, T. Endoh, H. Ohno, and T. Hanyu, *Standby-power-free compact ternary content-addressable memory cell chip using magnetic tunnel junction devices*, Applied Physics Express **2**, 023004 (2009).
 - ⁵ K. Nagasaka, *CPP-GMR technology for magnetic read heads of future high-density recording systems*, J. Magn. Magn. Mater. **321**, 508 (2009).
 - ⁶ D.D. Awschalom and Michael Flatté. *Challenges for semiconductor spintronics*, Nature Physics **3**, 153 (2007).
 - ⁷ Y. Kajiwara, K. Harii, S. Takahashi, J. Ohe, K. Uchida, M. Mizuguchi, H. Umezawa, H. Kawai, K. Ando, K. Takanashi, S. Maekawa & E. Saitoh, *Transmission of electrical signals by spin-wave interconversion in a magnetic insulator*, Nature **464**, 262 (2010).
 - ⁸ L. Berger, *Emission of spin waves by a magnetic multilayer traversed by a current*, Phys. Rev. B **54**, 9353 (1996).
 - ⁹ J. C. Slonczewski, *Current-driven excitation of magnetic multilayers*, J. Magn. Magn. Mater. **159**, L1 (1996).
 - ¹⁰ M. Tsoi, A. G. M. Jansen, J. Bass, W. C. Chiang, M. Seck, V. Tsoi, and P. Wyder, *Excitation of a magnetic multilayer by an electric current*, Phys. Rev. Lett. **81**, 493 (1998).
 - ¹¹ E. B. Myers, D. C. Ralph, J. A. Katine, R. N. Louie, and R. A. Buhrman, *Current-induced switching in magnetic multilayer devices*, Science **285**, 867 (1999).
 - ¹² A. Janossy and P. Monod, *Spin waves for single electrons in paramagnetic metals*, Phys. Rev. Lett. **37**, 612 (1976).
 - ¹³ R. H. Silsbee, A. Janossy, and P. Monod, *Coupling between ferromagnetic and conduction-spin-resonance modes at a ferromagnet-normal-metal interface*, Phys. Rev. B **19**, 4382 (1979).
 - ¹⁴ Y. Tserkovnyak, A. Brataas, and G. E. W. Bauer, *Enhanced Gilbert damping in thin ferromagnetic films*, Phys. Rev. Lett. **88**, 117601 (2002).
 - ¹⁵ Y. Tserkovnyak, A. Brataas, G. E. W. Bauer, and B. I. Halperin, *Nonlocal magnetization dynamics in ferromagnetic heterostructures*, Rev. Mod. Phys. **77**, 1375 (2005).
 - ¹⁶ S. Mizukami, Y. Ando, and T. Miyazaki, *The Study on Ferromagnetic Resonance Linewidth for NM/80NiFe/NM (NM=Cu, Ta, Pd and Pt) Films*, Jpn. J. Appl. Phys. **40**, 580 (2001); S. Mizukami, Y. Ando, and T. Miyazaki, *Effect of spin diffusion on Gilbert damping for a very thin permalloy layer in Cu/permalloy/Cu/Pt film*, Phys. Rev. B **66**, 104413 (2002).
 - ¹⁷ R. Urban, G. Woltersdorf, and B. Heinrich, *Gilbert damping in Single and Multilayer Ultrathin Films: Role of Interfaces in Nonlocal Spin Dynamics*, Phys. Rev. Lett. **87**, 217204 (2001).
 - ¹⁸ B. Heinrich, Y. Tserkovnyak, G. Woltersdorf, A. Brataas, R. Urban, and G. E. W. Bauer, *Dynamic Exchange Coupling in Magnetic Bilayers*, Phys. Rev. Lett. **90**, 187601 (2003).
 - ¹⁹ A. Brataas, G. E. W. Bauer, and P. J. Kelly, *Non-collinear magnetoelectronics*, Phys. Rep. **427**, 157 (2006).
 - ²⁰ D. C. Ralph and M. D. Stiles, *Spin transfer torques*, J. Magn. Magn. Materials **320**, 1190 (2008).
 - ²¹ A. Brataas, Yu. V. Nazarov, and G. E. W. Bauer, *Finite-element theory of transport in ferromagnet-normal metal systems*, Phys. Rev. Lett. **84**, 2481 (2000); *Spin-transport in multi-terminal normal metal-ferromagnet systems with non-collinear magnetizations*, Eur. Phys. J. B **22**, 99 (2001).
 - ²² X. Waintal, E. B. Myers, P. W. Brouwer, and D. C. Ralph, *Role of spin-dependent interface scattering in generating current-induced torques in magnetic multilayers*, Phys. Rev. B **62**, 12317 (2000).
 - ²³ G. E. W. Bauer, Y. Tserkovnyak, D. Huertas-Hernando, and A. Brataas, *Universal angular magnetoresistance and spin torque in ferromagnetic/normal metal hybrids*, Phys. Rev. B **67**, 094421 (2003).
 - ²⁴ V. S. Rychkov, S. Borlenghi, H. Jaffres, A. Fert, and X. Waintal, *Spin torque and waviness in magnetic multilayers: A bridge between Valet-Fert theory and quantum approaches*, Phys. Rev. Lett. **103**, 066602 (2009).
 - ²⁵ J.Z. Sun and D.C. Ralph, *Magnetoresistance and spin-transfer torque in magnetic tunnel junctions*, J. Magn. Magn. Mater. **320**, 1227 (2008).
 - ²⁶ S. S. P. Parkin, M. Hayashi, L. Thomas, *Magnetic Domain-Wall Racetrack Memory*, Science **320**, 190 (2008).
 - ²⁷ S. Zhang and Z. Li, *Roles of nonequilibrium conduction electrons on the magnetization dynamics of ferromagnets*, Phys. Rev. Lett. **93**, 127204 (2004).
 - ²⁸ S. E. Barnes and S. Maekawa, *Generalization of Faraday's law to include nonconservative spin forces*, Phys. Rev. Lett. **98**, 246601 (2007).
 - ²⁹ G. Tatara., H. Kohno, and J. Shibata, *Microscopic approach to current-driven domain wall dynamics*, Phys. Rep. **468**, 213 (2008).
 - ³⁰ G.S.D. Beach, M. Tsoi, J.L. Erskine, *Current-induced domain wall motion*, J. Magn. Magn. Mater. **320**, 1272 (2008).
 - ³¹ Y. Tserkovnyak and M. Mecklenburg, *Electron transport driven by nonequilibrium magnetic textures*, Phys. Rev. B **77**, 134407 (2008).
 - ³² K. M. D. Hals, A. K. Nguyen, and A. Brataas, *Intrinsic coupling between current and domain wall motion in (Ga,Mn)As*,

- Phys. Rev. Lett. **102**, 256601 (2009).
- ³³ G. E. W. Bauer, S. Bretzel, A. Brataas, and Y. Tserkovnyak, *Nanoscale magnetic heat pumps and engines*, Phys. Rev. B **81**, 024427 (2010).
- ³⁴ S. R. de Groot, *Thermodynamics of irreversible processes* (Interscience, New York, 1952).
- ³⁵ S. J. Barnett, *Magnetization by Rotation*, Phys. Rev. **6**, 239 (1915); S. J. Barnett, *Gyromagnetic and Electron-Inertia Effects*, Rev. Mod. Phys. **7**, 129 (1935).
- ³⁶ A. Einstein and W. J. de Haas, *Experimenteller Nachweis der Ampereschen Molekularströme*, Deutsche Physikalische Gesellschaft, Verhandlungen **17**, 152 (1915).
- ³⁷ J. Grollier, V. Cros, A. Hamzic, J. M. George, H. Jaffres, A. Fert, G. Faini, J. Ben Youssef, and H. Legall, *Spin-polarized current induced switching in Co/Cu pillars*, Appl. Phys. Lett. **78**, 3663 (2001).
- ³⁸ S. I. Kiselev, J. C. Sankey, I. N. Krivorotov, N. C. Emley, R. J. Schoelkopf, R. A. Buhrman, and D. C. Ralph, *Microwave oscillations of a nanomagnet driven by a spin-polarized current*, Nature **425**, 380 (2003).
- ³⁹ B. Ozyilmaz, A. D. Kent, D. Monsma, J. Z. Sun, M. J. Rooks, and R. H. Koch, *Current-induced magnetization reversal in high magnetic field in Co/Cu/Co nanopillars*, Phys. Rev. Lett. **91**, 067203 (2003).
- ⁴⁰ I. N. Krivorotov, N. C. Emley, J. C. Sankey, S. I. Kiseev, D. C. Ralphs, and R. A. Buhrman, *Time-domain measurements of nanomagnet dynamics driven by spin-transfer torques*, Science **307**, 228 (2005).
- ⁴¹ Y. T. Cui, G. Finocchio, C. Wang, J. A. Katine, R. A. Buhrman, and D. C. Ralph, *Single-shot time-domain studies of spin-torque-driven switching in magnetic tunnel junctions*, Phys. Rev. Lett. **104**, 097201 (2010).
- ⁴² K. M. D. Hals, Arne Brataas, and Y. Tserkovnyak, *Scattering theory of charge-current-induced magnetization dynamics*, EPL **90**, 4702 (2010).
- ⁴³ A. A. Kovalev, A. Brataas, and G. E. W. Bauer, *Spin-transfer in diffusive ferromagnet-normal metal systems with spin-flip scattering*, Phys. Rev. B **66**, 224424 (2002).
- ⁴⁴ A. Brataas, Y. Tserkovnyak, and G. E. W. Bauer, *Current-induced macrospin versus spin wave excitations in spin valves*, Phys. Rev. B **73**, 014408 (2006).
- ⁴⁵ M. Zwierzycki, Y. Tserkovnyak, P. J. Kelly, A. Brataas, and G. E. W. Bauer, *First-principles study of magnetization relaxation enhancement and spin transfer in thin magnetic films*, Phys. Rev. B **71**, 064420 (2005).
- ⁴⁶ A. A. Kovalev, G. E. W. Bauer, and A. Brataas, *Perpendicular spin valves with ultrathin ferromagnetic layers: Magneto-electronic circuit investigation of finite-size effects*, Phys. Rev. B **73**, 054407 (2006).
- ⁴⁷ S. E. Barnes, *The effect that finite lattice spacing has upon the ESR Bloch equations*, J. Phys. F: Met. Phys. **4**, 1535 (1974).
- ⁴⁸ M. Büttiker, H. Thomas, and A. Prêtre, *Current partition in multiprobe conductors in the presence of slowly oscillating external potentials*, Z. Phys. B **94**, 133 (1994).
- ⁴⁹ E. Saitoh, M. Ueda, H. Miyajima, and G. Tatara, *Conversion of spin current into charge current at room temperature: inverse spin-Hall effect*, Appl. Phys. Lett. **88**, 182509 (2006).
- ⁵⁰ F. D. Czeschka, L. Dreher, M. S. Brandt, M. Weiler, M. Althammer, I.-M. Imort, G. Reiss, A. Thomas, W. Schoch, W. Limmer, H. Huebl, R. Gross, S. T. B. Goennenwein, *Scaling behavior of the spin pumping effect in ferromagnet/platinum bilayers*, Phys. Rev. Lett. **107**, 046601 (2011).
- ⁵¹ G. E. Volovik, *Linear momentum in ferromagnets*, J. Phys. C, **L83** (1987).
- ⁵² G. Tatara and H. Kohno, *Theory of current-driven domain wall motion: spin transfer versus momentum transfer*, Phys. Rev. Lett. **92**, 086601 (2004).
- ⁵³ A. Thiaville, *Micromagnetic understanding of current-driven domain wall motion in patterned nanowires*, EPL **69**, 990 (2005).
- ⁵⁴ R. A. Duine, *Spin pumping by a field-driven domain wall*, Phys. Rev. B **77**, 014409 (2008).
- ⁵⁵ G. E. W. Bauer, A. H. MacDonald, and S. Maekawa, *Spin Caloritronics*, Solid State Comm. **150**, 459 (2010).
- ⁵⁶ A. Brataas, Y. Tserkovnyak, G. E. W. Bauer, and B. I. Halperin, *Spin battery operated by ferromagnetic resonance*, Phys. Rev. B **66**, 060404 (2002).
- ⁵⁷ M. V. Costache, M. Sladkov, S. M. Watts, C. H. van der Wal, and B. J. van Wees, *Electrical detection of spin pumping due to the precessing magnetization of a single ferromagnet*, Phys. Rev. Lett. **97**, 216603 (2006); M. V. Costache, S. M. Watts, C. H. van der Wal, and B. J. van Wees, *Electrical detection of spin pumping: dc voltage generated by ferromagnetic resonance at ferroamagnet/nonmagnet contact*, Phys. Rev. B **78**, 064423 (2008).
- ⁵⁸ X. Wang, G. E. W. Bauer, B. J. van Wees, A. Brataas, and Y. Tserkovnyak, *Voltage generation by ferromagnetic resonance at a nonmagnetic to ferromagnet contact*, Phys. Rev. Lett. **97**, 216602 (2006).
- ⁵⁹ K. Ando, S. Takahashi, J. Ieda, H. Kurebayashi, T. Trypiniotis, C. H. W. Barnes, S. Maekawa, and E. Saitoh, *Electrically tunable spin injector free from the impedance mismatch problem*, Nature Materials, Advanc Online Publicatino, 26. June 2011.
- ⁶⁰ J. Foros, A. Brataas, Y. Tserkovnyak, and G. E. W. Bauer, *Current-induced noise and damping in nonuniform ferromagnets*, Phys. Rev. B **78**, 140402 (2008).
- ⁶¹ S. Zhang and S. S.-L. Zhang, *Generalization of the Landau-Lifshitz-Gilbert equation for conducting ferromagnets*, Phys. Rev. Lett. **102**, 086601 (2009).
- ⁶² C. H. Wong and Y. Tserkovnyak, *Dissipative dynamics of magnetic solitons in metals*, Phys. Rev. B **81**, 060404 (2010).
- ⁶³ J. Foros, A. Brataas, Y. Tserkovnyak, and G. E. W. Bauer, *Magnetization noise in magnetoelectronic nanostructures*, Phys. Rev. Lett. **95**, 016601 (2005).
- ⁶⁴ M. Hatami, G. E. W. Bauer, Q. Zhang, and J. Kelly, *Thermal Spin-Transfer Torque in Magnetoelectronic Devices*, Phys. Rev. Lett. **99**, 066603 (2007).
- ⁶⁵ A. A. Kovalev and Y. Tserkovnyak, *Thermoelectric spin transfer in textured magnets*, Phys. Rev. B **80**, 100408 (2009).

- ⁶⁶ K. M. Schep, J. B. A. N. van Hoof, P. J. Kelly, G. E. W. Bauer, and J. E. Inglesfield, *Interface resistances of magnetic multilayers*, Phys. Rev. B **56**, 10805–10808 (1997).
- ⁶⁷ M. Büttiker, *Scattering theory of current and intensity noise correlations in conductors and waveguides*, Phys. Rev. B **46**, 12485 (1992).
- ⁶⁸ Y. Tserkovnyak, H. J. Skadsem, A. Brataas, and G. E. W. Bauer, *Current-induced magnetization dynamics in disordered itinerant ferromagnets*, Phys. Rev. B **74**, 144405 (2006).
- ⁶⁹ H. Kohno and G. Tatara, *Microscopic calculation of spin torques in disordered ferromagnets*, J. Phys. Soc. Jpn, **75**, 113706 (2006).
- ⁷⁰ R. A. Duine, A. S. Núñez, J. Sinova, and A. H. MacDonald, *Functional keldysh theory of spin torques*, Phys. Rev. B **75**, 214420 (2007).
- ⁷¹ S. E. Barnes and S. Maekawa, *Current-spin coupling for ferromagnetic domain walls in fine wires*, Phys. Rev. Lett. **95**, 107204 (2005).
- ⁷² N. L. Schryer and L. R. Walker, *The motion of 180 degree domain walls in uniform dc magnetic fields*, J. Appl. Phys. **45**, 5406 (1974).
- ⁷³ Y. Tserkovnyak, A. Brataas, and G. E. Bauer, *Theory of current-driven magnetization dynamics in inhomogeneous ferromagnets*, J. Magn. Magn. Mater. **320**, 1282 (2008).
- ⁷⁴ H. J. Skadsem, Y. Tserkovnyak, A. Brataas, and G. E. W. Bauer, *Magnetization damping in a local-density approximation*, Phys. Rev. B **75**, 094416 (2007).
- ⁷⁵ E. Runge and E. K. U. Gross, *Density-functional theory for time-dependent systems*, Phys. Rev. Lett. **52**, 997 (1984).
- ⁷⁶ K. Capelle, G. Vignale, and B. L. Györfy, *Spin currents and spin dynamics in time-dependent density-functional theory*, Phys. Rev. Lett. **87**, 206403 (2001).
- ⁷⁷ Z. Qian and G. Vignale, *Spin dynamics from time-dependent spin-density-functional theory*, Phys. Rev. Lett. **88**, 056404 (2002).
- ⁷⁸ I. Garate, K. Gilmore, M. D. Stiles, and A. H. MacDonald, *Nonadiabatic spin-transfer torque in real materials*, Phys. Rev. B **79**, 104416 (2009).
- ⁷⁹ Y. Tserkovnyak, G. A. Fiete, and B. I. Halperin, *Mean-field magnetization relaxation in conducting ferromagnets*, Appl. Phys. Lett. **84**, 5234 (2004).
- ⁸⁰ M. Büttiker, H. Thomas, and A. Prêtre, *Current partition in multiprobe conductors in the presence of slowly oscillating external potentials*, Z. Phys. B **94**, 133 (1994).
- ⁸¹ P. W. Brouwer, *Scattering approach to parametric pumping*, Phys. Rev. B **58**, R10135 (1998).
- ⁸² A. Chernyshov, M. Overby, X. Liu, J. K. Furdyna, Y. Lyanda-Geller, and L. P. Rokhinson, *Evidence for reversible control of magnetization in a ferromagnetic material by means of spin-orbit magnetic field*, Nature Phys. **5**, 656 (2009).
- ⁸³ A. Manchon and S. Zhang, *Theory of nonequilibrium intrinsic spin torque in a single nanomagnet*, Phys. Rev. B **78**, 212405 (2008).
- ⁸⁴ I. Garate and A. H. MacDonald, *Influence of a transport current on magnetic anisotropy in gyrotropic ferromagnets*, Phys. Rev. B **80**, 134403 (2009).
- ⁸⁵ J. E. Avron, A. Elgart, G. M. Graf, and L. Sadun, *Optimal quantum pumps*, Phys. Rev. Lett. **87**, 236601 (2001).
- ⁸⁶ M. Moskalets and M. Büttiker, *Dissipation and noise in adiabatic quantum pumps*, Phys. Rev. B **66**, 035306 (2002).
- ⁸⁷ M. Moskalets and M. Büttiker, *Floquet scattering theory of quantum pumps*, Phys. Rev. B **66**, 205320 (2002).
- ⁸⁸ A. Brataas, Y. Tserkovnyak, and G. E. W. Bauer, *Scattering theory of Gilbert damping*, Phys. Rev. Lett. **101**, 037207 (2008).
- ⁸⁹ A. A. Starikov, P. J. Kelly, A. Brataas, Y. Tserkovnyak, and G. E. W. Bauer, *A unified first-principles study of gilbert damping, spin-flip diffusion and resistivity in transition metal alloys*, Phys. Rev. Lett. **105**, 236602 (2010).
- ⁹⁰ Z. Li and S. Zhang, *Domain-wall dynamics driven by adiabatic spin-transfer torques*, Phys. Rev. B **70**, 024417 (2004).
- ⁹¹ K. Xia, P. J. Kelly, G. E. W. Bauer, A. Brataas, and I. Turek, *Spin torques in ferromagnetic/normal-metal structures*, Phys. Rev. B **65**, 220401 (2002).
- ⁹² K. Carva and I. Turek, *Spin-mixing conductances of thin magnetic films from first principles*, Phys. Rev. B **76**, 104409 (2007).
- ⁹³ M. D. Stiles and A. Zangwill, *Anatomy of spin-transfer torque*, Phys. Rev. B **66**, 014407 (2002).
- ⁹⁴ A. Brataas, G. Zaránd, Y. Tserkovnyak, and G. E. W. Bauer, *Magnetoelectronic spin echo*, Phys. Rev. Lett. **91**, 166601 (2003).
- ⁹⁵ B. Heinrich, D. Fraitová, and V. Kamberský, *The influence of s-d exchange on relaxation of magnons in metals*, Phys. Stat. Sol. B **23**, 501–507 (1967).
- ⁹⁶ V. Kamberský, *Ferromagnetic resonance in iron whiskers*, Can. J. Phys. **48**, 1103 (1970).
- ⁹⁷ V. Korenman and R. E. Prange, *Anomalous damping of spin waves in magnetic metals*, Phys. Rev. B **6**, 2769 (1972).
- ⁹⁸ J. Kuneš and V. Kamberský, *First-principles investigation of the damping of fast magnetization precession in ferromagnetic 3d metals*, Phys. Rev. B **65**, 212411 (2002).
- ⁹⁹ B. Heinrich, *Spin relaxation in magnetic metallic layers and multilayers*, Ultrathin magnetic structures III (J. A. C. Bland and B. Heinrich, eds.), Springer, New York, 2005, pp. 143–210.
- ¹⁰⁰ V. Kamberský, *On ferromagnetic resonance damping in metals*, Czech. J. Phys. **26**, 1366–1383 (1976).
- ¹⁰¹ K. Gilmore, Y. U. Idzerda, and M. D. Stiles, *Identification of the dominant precession-damping mechanism in Fe, Co, and Ni by first-principles calculations*, Phys. Rev. Lett. **99**, 027204 (2007).
- ¹⁰² K. Gilmore, Y. U. Idzerda, and M. D. Stiles, *Spin-orbit precession damping in transition metal ferromagnets*, J. Appl. Phys. **103**, 07D303 (2008).

- ¹⁰³ K. Gilmore, M. D. Stiles, J. Seib, D. Steiauf, and M. Fähnle, *Anisotropic damping of the magnetization dynamics in Ni, Co, and Fe*, Phys. Rev. B **81**, 174414 (2010).
- ¹⁰⁴ V Kamberský, *Spin-orbital Gilbert damping in common magnetic metals*, Phys. Rev. B **76**, 134416 (2007).
- ¹⁰⁵ K. Xia, P. J. Kelly, G. E. W. Bauer, I. Turek, J. Kudrnovský, and V. Drchal, *Interface resistance of disordered magnetic multilayers*, Phys. Rev. B **63**, 064407 (2001).
- ¹⁰⁶ K. Xia, M. Zwierzycki, M. Talanana, P. J. Kelly, and G. E. W. Bauer, *First-principles scattering matrices for spin-transport*, Phys. Rev. B **73**, 064420 (2006).
- ¹⁰⁷ T. Ando, *Quantum point contacts in magnetic fields*, Phys. Rev. B **44**, 8017–8027 (1991).
- ¹⁰⁸ O. K. Andersen, *Linear methods in band theory*, Phys. Rev. B **12**, 3060–3083 (1975).
- ¹⁰⁹ O. K. Andersen, Z. Pawłowska, and O. Jepsen, *Illustration of the linear-muffin-tin-orbital tight-binding representation: Compact orbitals and charge density in Si*, Phys. Rev. B **34**, 5253–5269 (1986).
- ¹¹⁰ I. Turek, V. Drchal, J. Kudrnovský, M. Šob, and P. Weinberger, *Electronic structure of disordered alloys, surfaces and interfaces*, Kluwer, Boston-London-Dordrecht, 1997.
- ¹¹¹ P. Soven, *Coherent-potential model of substitutional disordered alloys*, Phys. Rev. **156**, 809–813 (1967).
- ¹¹² M. Büttiker, Y. Imry, R. Landauer, and S. Pinhas, *Generalized many-channel conductance formula with application to small rings*, Phys. Rev. B **31**, 6207–6215 (1985).
- ¹¹³ S. Datta, *Electronic transport in mesoscopic systems*, Cambridge University Press, Cambridge, 1995.
- ¹¹⁴ J. Smit, *Magneto-resistance of ferromagnetic metals and alloys at low temperatures*, Physica **17**, 612–627 (1951).
- ¹¹⁵ T. R. McGuire and R. I. Potter, *Anisotropic magneto-resistance in ferromagnetic 3d alloys*, IEEE Trans. Mag. **11**, 1018–1038 (1975).
- ¹¹⁶ O. Jaoul, I. Campbell, and A. Fert, *Spontaneous resistivity anisotropy in Ni alloys*, J. Magn. & Magn. Mater. **5**, 23–34 (1977).
- ¹¹⁷ M. C. Cadeville and B. Loegel, *On the transport properties in concentrated Ni-Fe alloys at low temperatures*, J. Phys. F: Met. Phys. **3**, L115–L119 (1973).
- ¹¹⁸ J. Banhart, H. Ebert, and A. Vernes, *Applicability of the two-current model for systems with strongly spin-dependent disorder*, Phys. Rev. B **56**, 10165–10171 (1997).
- ¹¹⁹ J. Banhart and H. Ebert, *First-principles theory of spontaneous-resistance anisotropy and spontaneous hall effect in disordered ferromagnetic alloys*, Europhys. Lett. **32**, 517–522 (1995).
- ¹²⁰ S. Mizukami, Y. Ando, and T. Miyazaki, *Ferromagnetic resonance linewidth for NM/80NiFe/NM films (NM=Cu, Ta, Pd and Pt)*, J. Magn. & Magn. Mater. **226–230**, 1640 (2001).
- ¹²¹ S. Mizukami, Y. Ando, and T. Miyazaki, *The study on ferromagnetic resonance linewidth for NM/80NiFe/NM (NM = Cu, Ta, Pd and Pt) films*, Jpn. J. Appl. Phys. **40**, 580–585 (2001).
- ¹²² W. Bailey, P. Kabos, F. Mancoff, and S. Russek, *Control of magnetization dynamics in Ni₈₁Fe₁₉ thin films through the use of rare-earth dopants*, IEEE Trans. Mag. **37**, 1749–1754 (2001).
- ¹²³ C. E. Patton, Z. Frait, and C. H. Wilts, *Frequency dependence of the parallel and perpendicular ferromagnetic resonance linewidth in Permalloy films, 2–36 GHz*, J. Appl. Phys. **46**, 5002–5003 (1975).
- ¹²⁴ S. Ingvarsson, G. Xiao, S.S.P. Parkin, and R.H. Koch, *Tunable magnetization damping in transition metal ternary alloys*, Appl. Phys. Lett. **85**, 4995–4997 (2004).
- ¹²⁵ H Nakamura, Yasuo Ando, S Mizukami, and H Kubota, *Measurement of magnetization precession for NM/Ni₈₀Fe₂₀/NM (NM= Cu and Pt) using time-resolved Kerr effect*, Jpn. J. Appl. Phys. **43**, L787–L789 (2004).
- ¹²⁶ J. O. Rantschler, B. B. Maranville, J. J. Mallett, P. Chen, R. D. McMichael, and W. F. Egelhoff, *Damping at normal metal/Permalloy interfaces*, IEEE Trans. Mag. **41**, 3523–3525 (2005).
- ¹²⁷ R. Bonin, M. L. Schneider, T. J. Silva, and J. P. Nibarger, *Dependence of magnetization dynamics on magnetostriction in NiFe alloys*, J. Appl. Phys. **98**, 123904 (2005).
- ¹²⁸ L. Lagae, R. Wirix-Speetjens, W. Eyckmans, S. Borghs, and J. de Boeck, *Increased Gilbert damping in spin valves and magnetic tunnel junctions*, J. Magn. & Magn. Mater. **286**, 291–296 (2005).
- ¹²⁹ J. P. Nibarger, R. Lopusnik, Z. Celinski, and T. J. Silva, *Variation of magnetization and the Landé g factor with thickness in Ni-Fe films*, Appl. Phys. Lett. **83**, 93–95 (2003).
- ¹³⁰ N Inaba, H Asanuma, S Igarashi, S Mori, F Kirino, K Koike, and H Morita, *Damping constants of Ni-Fe and Ni-Co alloy thin films*, IEEE Trans. Mag. **42**, 2372–2374 (2006).
- ¹³¹ M. Oogane, T. Wakitani, S. Yakata, R. Yilgin, Y. Ando, A. Sakuma, and T. Miyazaki, *Magnetic damping in ferromagnetic thin films*, Jpn. J. Appl. Phys. **45**, 3889–3891 (2006).
- ¹³² S. M. Bhagat and P. Lubitz, *Temperature variation of ferromagnetic relaxation in the 3d transition metals*, Phys. Rev. B **10**, 179–185 (1974).
- ¹³³ B. Heinrich, D. J. Meredith, and J. F. Cochran, *Wave number and temperature-dependent Landau-Lifshitz damping in Nickel*, J. Appl. Phys. **50**, 7726–7728 (1979).
- ¹³⁴ D Bastian and E Biller, *Damping of ferromagnetic resonance in Ni-Fe alloys*, Phys. Stat. Sol. A **35**, 113–120 (1976).
- ¹³⁵ J. Xiao, A. Zangwill, and M. D. Stiles, *Spin-transfer torque for continuously variable magnetization*, Phys. Rev. B **73**, 054428 (2006).
- ¹³⁶ J.-P. Adam, N. Vernier, J. Ferré, A. Thiaville, V. Jeudy, A. Lemaitre, L. Thevenard, and G. Faini, *Nonadiabatic spin-transfer torque in (Ga,Mn)As with perpendicular anisotropy*, Phys. Rev. B **80**, 193204 (2009).
- ¹³⁷ C. Burrowes, A. P. Mihai, D. Ravelosona, J.-V. Kim, C. Chappert, L. Vila, A. Marty, Y. Samson, F. Garcia-Sanchez, L. D. Buda-Prejbeanu, I. Tudosa, E. E. Fullerton, and J.-P. Attané, *Non-adiabatic spin-torques in narrow magnetic domain walls*, Nature Physics **6**, 17–21 (2010).
- ¹³⁸ M. Eltschka, M. Wötzel, J. Rhensius, S. Krzyk, U. Nowak, M. Kläui, T. Kasama, R. E. Dunin-Borkowski, L. J. Heyderman,

- H. J. van Driel, and R. A. Duine, *Nonadiabatic spin torque investigated using thermally activated magnetic domain wall dynamics*, Phys. Rev. Lett. **105**, 056601 (2010).
- ¹³⁹ M. Hayashi, L. Thomas, C. Rettner, R. Moriya, and S. S. P. Parkin, *Dynamics of domain wall depinning driven by a combination of direct and pulsed currents*, Appl. Phys. Lett. **92**, 162503 (2008).
- ¹⁴⁰ S. Lepadatu, J. S. Claydon, C. J. Kinane, T. R. Charlton, S. Langridge, A. Potenza, S. S. Dhesi, P. S. Keatley, R. J. Hicken, B. J. Hickey, and C. H. Marrows, *Domain-wall pinning, nonadiabatic spin-transfer torque, and spin-current polarization in Permalloy wires doped with Vanadium*, Phys. Rev. B **81**, 020413 (2010).
- ¹⁴¹ S. Lepadatu, A. Vanhaverbeke, D. Atkinson, R. Allenspach, and C. H. Marrows, *Dependence of domain-wall depinning threshold current on pinning profile*, Phys. Rev. Lett. **102**, 127203 (2009).
- ¹⁴² T. A. Moore, M. Kläui, L. Heyne, P. Möhrke, D. Backes, J. Rhensius, U. Rüdiger, L. J. Heyderman, J.-U. Thiele, G. Woltersdorf, C. H. Back, A. Fraile Rodríguez, F. Nolting, T. O. Mentès, M. Á. Niño, A. Locatelli, A. Potenza, H. Marchetto, S. Cavill, and S. S. Dhesi, *Scaling of spin relaxation and angular momentum dissipation in Permalloy nanowires*, Phys. Rev. B **80**, 132403 (2009).
- ¹⁴³ G. Tatara, H. Kohno, and J. Shibata, *Microscopic approach to current-driven domain wall dynamics*, Phys. Rep. **468**, 213–301 (2008).
- ¹⁴⁴ A. Ghosh, J. F. Sierra, S. Auffret, U. Ebels, and W. E. Bailey, *Dependence of nonlocal Gilbert damping on the ferromagnetic layer type in ferromagnet/Cu/Pt heterostructures*, Appl. Phys. Lett. **98**, 052508 (2011).
- ¹⁴⁵ C. W. Sandweg, Y. Kajiwara, A. C. Chumak, A. A. Serga, V. I. Vasyuchka, M. B. Jungfleisch, E. Saitoh, and B. Hillebrands, *Spin pumping by parametrically excited exchange magnons*, Phys. Rev. Lett. **106**, 216601 (2011).
- ¹⁴⁶ M. Hayashi, L. Thomas, Ya. B. Bazaliy, C. Rettner, R. Moriya, X. Jiang, and S. S. P. Parkin, *Influence of Current on Field-Driven Domain Wall Motion in Permalloy Nanowires from Time Resolved Measurements of Anisotropic Magnetoresistance*, Phys. Rev. Lett. **96**, 197207 (2006).
- ¹⁴⁷ G. Meier, M. Bolte, R. Eiselt, B. Krüger, D.-H. Kim, and P. Fischer, *Direct Imaging of Stochastic Domain-Wall Motion Driven by Nanosecond Current Pulses*, Phys. Rev. Lett. **98**, 187202 (2007).
- ¹⁴⁸ L. Thomas, M. Hayashi, X. Jiang, R. Moriya, C. Rettner, and S. S. P. Parkin, *Oscillatory dependence of current-driven magnetic domain wall motion on current pulse length*, Nature **443**, 197 (2006).
- ¹⁴⁹ L. Heyne, M. Kläui, D. Backes, T. A. Moore, S. Krzyk, U. Rüdiger, L. J. Heyderman, A. F. Rodríguez, F. Nolting, T. O. Mentès, M. Á. Niño, A. Locatelli, K. Kirsch, and R. Mattheis, *Relationship between nonadiabaticity and damping in permalloy studied by current induced spin structure transformations*, Phys. Rev. Lett. **100**, 066603 (2008).
- ¹⁵⁰ S. Lepadatu, J. S. Claydon, C. J. Kinane, T. R. Charlton, S. Langridge, A. Potenza, S. S. Dhesi, P. S. Keatley, R. J. Hicken, B. J. Hickey, and C. H. Marrows, *Domain-wall pinning, nonadiabatic spin-transfer torque, and spin-current polarization in permalloy wires doped with vanadium*, Phys. Rev. B **81**, 020413(R) (2010).
- ¹⁵¹ B. Krüger, M. Najafi, S. Bohlens, R. Frömter, D. P. F. Möller, and D. Pfannkuche, *Proposal of a Robust Measurement Scheme for the Nonadiabatic Spin Torque Using the Displacement of Magnetic Vortices*, Phys. Rev. Lett. **104**, 077201 (2010).
- ¹⁵² L. Heyne, J. Rhensius, D. Ilgaz, A. Bisig, U. Rüdiger, M. Kläui, L. Joly, F. Nolting, L. J. Heyderman, J. U. Thiele, and F. Kronas, *Direct Determination of Large Spin-Torque Nonadiabaticity in Vortex Core Dynamics*, Phys. Rev. Lett. **105**, 187203 (2010).
- ¹⁵³ M. Eltschka, M. Wötzel, J. Rhensius, S. Krzyk, U. Nowak, M. Kläui, T. Kasama, R. E. Dunin-Borkowski, L. J. Heyderman, H. J. van Driel, and R. A. Duine, *Non-adiabatic spin torque investigated using thermally activated magnetic domain wall dynamics*, Phys. Rev. Lett. **105**, 056601 (2010).
- ¹⁵⁴ C. Burrowes, A. P. Mihai, D. Ravelosona, J.-V. Kim, C. Chappert, L. Vila, A. Marty, Y. Samson, F. Garcia-Sanchez, L. D. Buda-Prejbeanu, I. Tudosa, E. E. Fullerton & J.-P. Attané, *Non-adiabatic spin-torques in narrow magnetic domain walls*, Nat. Phys. **6**, 17 (2010)
- ¹⁵⁵ M. Yamanouchi, J. Ieda, F. Matsukura, S. E. Barnes, S. Maekawa, and H. Ohno, *Universality classes for domain wall motion in the ferromagnetic semiconductor*, Science **317**, 1726 (2007).
- ¹⁵⁶ S. A. Yang, G. S. D. Beach, C. Knutson, D. Xiao, Q. Niu, M. Tsoi, and J. L. Erskine, *Universal electromotive force induced by domain wall motion*, Phys. Rev. Lett. **102**, 067201 (2009).